The Effects of a Calcineurin Inhibitor on Muscle Fibre Type and the Pathology of Centronuclear Myopathy in *Pln*^{OE} Mice

by

Paige Jilleia Chambers

A thesis
presented to the University of Waterloo
in fulfillment of the
thesis requirement for the degree of
Master of Science
in
Kinesiology

Waterloo, Ontario, Canada, 2017

Author's Declaration

I hereby declare that I am the sole author of this thesis. This is a true copy of the thesis, including any required final revisions, as accepted by my examiners.

I understand that my thesis may be made electronically available to the public.

Abstract

The sarco(endo)plasmic reticulum Ca^{2+} ATPase (SERCA) pump is responsible for pumping calcium from the cytosol back into the lumen of the sarcoplasmic reticulum post contraction. SERCA activity can be reduced by an inhibitory protein, phospholamban (PLN), which binds directly to the pump. Interestingly, overexpressing PLN in transgenic mice (Pln^{OE}) creates a replica of centronuclear myopathy (CNM). CNM is a grouping of rare congenital diseases with three common muscular abnormalities: abundant central nuclei, centrally aggregated oxidative activity and type 1 fibre predominance. Calcineurin (CnA) is a Ca^{2+}-calmodulin dependent serine-threonine phosphatase, which is known to activate a signalling cascade leading to slow-twitch fibre gene expression. Upon activation by excess Ca^{2+}, CnA dephosphorylates nuclear factor of activated T-cells (NFAT) proteins, which then translocate to the nucleus where they act as transcription factors for slow-twitch fibre promotion. Western blotting of muscle lysates from Pln^{OE} mice showed increased CnA and nuclear NFAT content in slow twitch muscle, soleus and gluteus minimus, while no differences were found in the diaphragm which contains much less CNM disease symptoms. Therefore, this study examined the hypothesis that CnA activation may be driving the predominance of type I fibres and may be targeted as a potential therapeutic strategy to alleviate the CNM phenotype in Pln^{OE} mice. Here, developing (4 week old) and adult (4-6 month old) Pln^{OE} mice were treated with the CnA inhibitor, cyclosporin A (CsA), at 25mg/kg body weight twice a day for two weeks. Soleus muscles from vehicle and CsA treated mice were excised for histology and immunofluorescence to assess the CNM phenotype, Western blotting for protein content and whole muscle contractility to assess muscle function. CsA treatment blunted type I fibre predominance and promoted hybrid and type II fibres in both age groups. CsA treated adult Pln^{OE} mice were also found to have increased force,

decreased fibrosis, reduced PLN and sarcolipin content. CsA treatment did not eliminate central aggregations of oxidative activity or have an effect on the percentage of fibres displaying central nuclei suggesting these CNM features may not be connected to CnA activity. CnA content was reduced in the CsA treated animals but changes in CnA activity in this study are unclear as western blotting showed increased activity while immunofluorescence displayed decreased activity and less nuclear NFAT. Surprisingly, CsA treatment had minimal effects in developing Pln^{OE} mice with only small difference in fibre type observed between vehicle and CsA animals. In summary, CsA treatment provides modest improvements in fibre type, cellular phenotype and muscle function in adult Pln^{OE} animals however it has little effect on younger mice developing the disease. Targeting fibre type as a potential treatment for CNM merits further research to determine the appropriate timing for treatment, other potential pharmaceuticals that do not disrupt immune signalling or hypertrophy and the underlying mechanism by which the overexpression of PLN causes CNM.

Acknowledgements

First and foremost, I'd like to acknowledge my supervisor, Dr. Russell Tupling. Thank you for taking a leap of faith and welcoming me into your lab. Your endless support and positive attitude have made a huge difference in my graduate experience and I am excited to be entering into my PhD with you as my mentor. I hope that you are as proud to have me as your graduate student as I am to have you as a supervisor.

As well, I need to thank all of my lab mates past and present, Dan Gamu, Val Fajardo, Khanh Tran, Frenk Kwon, Cat Bellissimo, Emma Juracic, Riley Sonnenburg, and Brad the Undergrad. I could not have done this without your support, your guidance, your extra hands and sense of humour. I'd also like to specifically thank Eric Bombardier, Val and Dan for their patience and guidance at the start of my masters; you guys are the best. To all the other kin-phys grad students, especially Kristen Boonstra, Erin (Tina) Turner, Laura Wood-Bennett and Maureen Riddell, you all have made my time here thus far so enjoyable and I wish you all the best in your future.

Finally to my family and loved ones, I am dedicating this thesis to you. The support, love and endless amounts of financial assistance you've offered are the foundation I stand on everyday. None of this could have been done without you and no amount of thank you's are enough. Dad, Mom, GC & GT, Brittany (Brad & Avery), David and Greg, love you to the moon and back.

Table of Contents

List of Abbreviations

ATP – Adenosine Triphosphate
BIN1 – Amphiphysin-2
Ca^{2+} - Calcium
CnA – Calcineurin
CNM – Centronuclear Myopathy
CsA – Cyclosporin A
DHPR – Dyhydropyridine Receptor
DMD – Duchenne Muscular Dystrophy
DNM2 – Dynamin 2
GSK3 – Glycogen Synthase Kinase 3
HSP70 – Heat Shock Protein 70
MHC – Myosin Heavy Chain
MLN - Myoregulin
MTM1- Myotubularin 1
NFAT – Nuclear Factor of Activated T-Cells
NFAT-p- Phosphorylated Nuclear Factor of Activated T-Cells
PKA – Protein Kinase A
PLN – Phosphoslamban
SERCA – Sarco(endo)plasmic reticulum Calcium ATPase
SLN – Sarcolipin
SR – Sarcoplasmic Reticulum
RYR – Ryanodine Receptor
Veh- Vehicle

Introduction

Calcium (Ca^{2+}) is essential for the proper health, structure and function of skeletal muscle. In skeletal muscle, the sarcoplasmic reticulum (SR) is the main storage site for Ca^{2+}, where the Ca^{2+} concentration ($[Ca^{2+}]$) has been measured to be 20mM (*1*) creating a large gradient between the SR lumen and the cytosol where $[Ca^{2+}]$ is approximately 30-100nM (*2*). Upon stimulation via an action potential, the dihydropyridine receptors (DHPR) located along the T-tubule membrane activate Ca^{2+} release from the SR by the opening of ryanodine receptors (RYR) embedded within the transverse portion of the SR membrane. When released into the cytosol, Ca^{2+} binds to troponin C allowing for cross bridge formation between actin and myosin and force generation (reviewed by Dulhenty, 2006). Upon cessation of the stimulus, subsequent re-uptake of Ca^{2+} back into the SR by the sarco(endo)plasmic reticulum Ca^{2+}-ATPase (SERCA) pump initiates muscular relaxation. The cytosolic $[Ca^{2+}]$ at any time is critical to the proper function of a muscle cell and is tightly regulated. Therefore, impairments in Ca2+ regulatory proteins such as DHPR, RYR, SERCA, and other Ca^{2+} buffering proteins and organelles including calsequestrin, parvalbumin, and mitochondria, could lead to dysregulated Ca^{2+} handling and decrements in muscle function and health. In particular, much attention has been given to the role of SERCA dysfunction in several muscle diseases including Brody's disease, cardiomyopathy, and Duchenne muscular dystrophy (DMD) (*3-5*).

SERCA Pumps and Calcium Regulation

The SERCA pump is a large 110kDa SR trans-membrane pump. There are three main isoforms of the pump, SERCA1, SERCA2, and SERCA3, each with alternative splicing variants, encoded for by the genes *ATP2A1, ATP2A2* and *ATP3A3,* respectively (*6, 7*). Each SERCA

isoform and splice variant has a different expression pattern in tissues throughout the body; notable for this thesis are the splice variants SERCA1a expressed in fast glycolytic type II muscle and SERCA2a expressed in slow oxidative and cardiac muscles (*7*). Although there are little differences in kinetics between the different SERCA isoforms *in vitro* (*8*), the level of isoform expression *in vivo* has a large impact on Ca^{2+} dynamics. Lytton et al. (1992) found that SERCA protein content was up to five fold higher in type II fibres compared to type I fibres in rat skeletal muscle (*9*). The increase in SERCA content in type II fibres corresponds with the finding that basal SERCA activity was nearly three fold higher in human type II fibres than type I fibres(*10*). Together the increased SERCA content and activity produce the faster muscular relaxation attributed with type II muscle fibres.

Structurally, SERCA pumps can be broken down into four domains: 1) the A domain, also known as the actuator domain for Ca^{2+}; 2) the N domain, which contains the nucleotide binding site for ATP; 3) the P domain or the phosphorylation domain, which contains the 351 aspartate residue that becomes phosphorylated during SERCA's catalytic cycle;, and 4) the M domain, which contains the ten transmembrane α-helices wherein lie the two Ca^{2+} binding sites (*3, 11*). As mentioned previously, the role of the SERCA pump is to actively transport Ca^{2+} from the cytosol back into the lumen of the SR and this is done through large conformational changes in the A, N, P and M domains driven by ATP hydrolysis. Two major conformational states of SERCA have been identified: E1, in which, there is a high affinity for Ca^{2+} promoting ion binding within the cytosol, and E2, wherein a low affinity for Ca^{2+} allows for its dissociation into the SR lumen (*12*). Under optimal conditions, SERCA will load both Ca^{2+} binding sites and transport two Ca^{2+} ions per ATP hydrolyzed; however, there are several SERCA regulatory proteins, some of which may alter this optimal allosteric ratio.

SERCA Regulation

Both positive and negative regulators of SERCA activity have been discovered, which work through varying mechanisms. The two most studied regulators of SERCA are the small integral proteins, sarcolipin (SLN) and phospholamban (PLN). SLN and PLN (31 and 52 amino acids, respectively) bind directly to the Ca^{2+} binding site within the M2, M4, M6 and M9 transmembrane helices of SERCA (*13, 14*). When SLN or PLN are bound to SERCA, they inhibit SERCA activity by reducing its apparent affinity for Ca^{2+}(*15, 16*). Furthermore in skeletal muscle, SLN but not PLN has been shown to uncouple the transport of Ca^{2+} from ATP hydrolysis meaning more ATP would be needed to transport the same amount of Ca^{2+} into the SR lumen (*17, 18*). Classically these inhibitory proteins have been associated with differing SERCA isoforms, with SLN and PLN binding and inhibiting SERCA1a and SERCA2a, respectively(*16, 19*). However, recent evidence suggests the relationship between the differing SERCA isoforms and regulatory proteins may be more complex than originally hypothesized. Using human single fibre western blotting, Fajardo et al. (2013) found that although PLN may preferentially inhibit SERCA2a in type I fibres whereas SLN primarily inhibits SERCA1a in type II fibres, they have the ability to bind to both isoforms and are co-expressed in many fibres (*20*). This corresponds with previous research showing PLN and SLN have the ability to synergistically bind to a single SERCA pump causing super inhibition (*21*).

Recently Anderson et al. (2015) discovered two additional SERCA regulatory proteins, myoregulin (MLN) and the micropeptide, DWORF. MLN is a homologous protein to SLN and PLN, which was discovered in a non-coding region of RNA. MLN was shown to be expressed in all skeletal muscle fibre types and, similar to PLN and SLN, has the ability to directly interact

with and inhibit SERCA (*22*). DWORF, on the other hand, was shown to enhance SERCA activity by displacing inhibitor proteins such as SLN, PLN, and MLN(*23*).

Cellular processes also have the capacity to affect SERCA function. While transient redox signaling has been shown to stabilize PLN in oligomer formations, which increases SERCA activity and improves cardriomyocyte contraction (*24*), cellular stress can cause irreversible oxidization, nitrosylation and S-glutathionyltion which negatively affect SERCA function (*25*). As well, oxidative damage has been associated with age-related reductions in cardiac muscle function as aged rat cardiac muscles contain similar SERCA content to healthy counterparts but have an increase in oxidative damage(*26*). In lieu of this, heat shock protein 70 (HSP70), previously shown to be activated during oxidative stress, binds directly to SERCA, stabilizing the pump and maintaining SERCA function in the face of thermal stress *(27),* In accordance with this, HSP70 was also shown to be upregulated in DMD human biopsies, thought to be a compensatory mechanism to deal with the cytotoxic stress from the excessive intracellular Ca^{2+} associated with this myopathy(*28*).

This connection between SERCA disfunction and disease states is not uncommon. DMD, cardiomyopathy/cardiac failure and aging have all been linked to decreased SERCA function, through decreased expression of the pump itself, increased expression of inhibitory proteins, or damage to the pump (*26, 29, 30*). As such, the manipulation of SERCA content or targeting of SERCA regulatory proteins has promise as a potential therapeutic strategy to combat muscle disease, such as DMD. Overexpression of SERCA1a in *mdx* mice, the murine model for DMD, caused a decrease in intracellular [Ca^{2+}], reduced central nuclei counts and increased exercise capacity along with a reduction in other detrimental Ca^{2+} associated symptoms such as swollen mitochondria and calpain activation (*31*). The overexpression of heat shock protein 72

(HSP72) has also been shown to alleviate the mdx phenotype and improve contractility of diaphragm muscles via improved SERCA function(*32*). The effects of PLN on SERCA function have also been most extensively researched in cardiovascular health where its inhibition of SERCA2a in cardiac muscle has been associated with cardiomyopathy (*33-35*). Surprisingly, very little research has examined the role of PLN in skeletal muscle myopathy.

Phospholamban

As stated previously, PLN inhibits SERCA activity by direct binding which lowers SERCA's apparent affinity for Ca^{2+}. Inherently, PLN is found in both a monomer and pentamer form, with monomer PLN being the active inhibitor of SERCA (*36*). The purpose of the pentamer formation of PLN is less clear and claimed to be both a selective cation channel (*37*) as well as a sink for phosphorylated inactive PLN(*38*). PLN has three distinct phosphorylation sites which are each phosphorylated by different kinases; protein kinase C (PKC) at Ser10, cAMP dependent protein kinase A (PKA) at Ser16 and Ca^{2+}-calmodulin -dependent protein kinase (CaMKII) at Thr17 (*39*). Phosphorylation at any of these sites disassociates PLN from SERCA, relieves any inhibitory effects and in turn increases SERCA's Ca^{2+} affinity and SR Ca^{2+} uptake (*40*). Likewise, ablation of PLN in mice increases SERCA activity causing decreased time to peak pressure and relaxation in the heart (*41*), a 2 fold increase in cardiomyocyte shortening upon contraction (*42*), and a 25% decrease in the time to half relaxation in soleus (*43*).

Within cardiac muscle, the presence of PLN and its inhibition of SERCA2a activity is especially detrimental as excess cytosolic Ca^{2+} and delayed relaxation have been associated with reduced ventricular filling and stroke volume, as well as cardiac disease and heart failure (*4*). Correspondingly, phosphorylation of PLN has been shown to weaken its inhibition of SERCA2a (*44*), increasing the apparent Ca^{2+} affinity and enhancing relaxation during β-adrenergic

stimulation (*45, 46*). As well, mutations in PLN cause cases of human dilated cardiomyopathy associated with refractory based heart failure (*35*). This pattern is also witnessed in mouse models as PLN overexpression in murine cardiac muscle causes cardiac hypertrophy and heart failure due to the inability to clear cytosolic Ca^{2+} (*47, 48*).

Although there is evidence suggesting the relationship between inhibited Ca^{2+} cycling and myopathy exists in skeletal muscle as well, considerably less research has been done in contrast to cardiac muscle. Transgenic rabbits overexpressing PLN presented dystrophic features including extensive muscle wasting and fatty accumulation in slow twitch muscle fibres and were almost completely immobile by 6 months of age (*49*). A murine transgenic model, which overexpresses PLN (Pln^{OE}) specifically in slow twitch fibreswas originally described by Song et al. (*50*). Interestingly, this group found reduced contractility and muscle mass but reported no myopathic phenotype in these mice. In contrast, Fajardo et al. (2015) has since shown that this same transgenic model presents a drastic increase in SLN content, reduced SERCA activity and a severe myopathy phenotype most similar to centronuclear myopathy (CNM) (*51*).

Centronuclear Myopathy

Centronuclear Myopathy, also known as myotubular myopathy, was first reported by Spiro et al. in a 1966 in a case study analysis of muscle tissue from an adolescent boy with muscle weakness and wasting (*52*). Upon histological analysis of muscle biopsies, three main pathological symptoms were found, which included: an abundance of central nuclei, a central aggregation of oxidative activity, and a predominance of type I fibers. Based on these three features, Spiro et al. speculated that the muscle looked as though it was arrested in development and hence chose to refer to it as myotubular myopathy. Since then, several genetic mutations have been uncovered and the etiology of CNM has strayed from the "arrested development"

theory, leading to the more common use of the term CNM over myotubular myopathy. Additionally, several other histological features have been associated with CNM, such as increased intracellular fibrosis, radiating SR strands upon SDH staining, triad deformations suggesting impairments in excitation-contraction coupling, and the presence of "Necklace fibers" which are small fibers containing centralized nuclei surrounded by a ring of mitochondria, sarcoplasmic reticulum and glycogen granules have also been reported (*51, 53-55*). These additional features vary vastly depending on the genetic mutation origin and corresponding classification of CNM.

Typically, CNM is grouped into four classifications; autosomal recessive, autosomal dominant, X-linked recessive and sporadic random cases (*56*). The most common of the four types is X-linked recessive CNM, which is most often associated with a mutation in the myotubularin 1 (*mtm1*) gene within the X chromosome (*57*). As such, this form of CNM predominantly affects males with females only being a carrier of the mutation. The *mtm1* gene codes for the protein myotubularin, a phosphoinositide phosphatase known to be essential in endosomal trafficking (*58*). Clinically, X-linked CNM displays the most severe variation of the disease commonly resulting in neonatal death (*53, 59*). The autosomal dominant form of CNM is associated with varying mutations along the gene coding for dynamin 2 (*DNM2*), a GTPase that forms around the necks of vesiculating membranes providing force for constriction as well as regulating actin and mictrotubule cytoskeletal networks (*60*). Autosomal dominant CNM is characterized by a progressive phenotype with varying severity depending on the exact DNM2 missense mutation (*61-63*). The autosomal- recessive and sporadic cases of CNM vary vastly in genetic abnormalities and clinical phenotypes. Mutations in hJUMPY (*mtmr14*), amphiphysin (*bin*1), and ryanodine receptor (*ryr*1) genes have all been linked to autosomal recessive and

sporadic cases (*64-66*). Sporadic and autosomal recessive cases of CNM are quite rare and are genetically classified on a case-to-case or family case basis. As a grouping, this category of CNM generally show a milder phenotype with onset occurring from neonatal to adulthood and a progressive muscular degeneration (*67*).

Because of the variation in genetic mutations, CNM is heterozygous in respect to clinical presentation, cellular abnormalities and singling dysfunction. As such, there is not one clear mechanism behind the phenotype seen within this disease. Aside from the sporadic RYR1 mutation case, all of the above genetic mutations encode for proteins involved in membrane trafficking and endo/exocytosis; however, the link between these mutations and how they work to cause the CNM phenotype is still unclear.

In order to conduct research into CNM, several transgenic animal models have been researched, including *Bin1*-null zebrafish, *MTM1*-mutated Labrador retriever dogs and mice, and *microRNA133a*-null mice (*53, 68-70*). Previous characterization of the Pln^{OE} murine model of CNM by our lab revealed the three hallmarks of the disease previously mentioned as well as reduced muscle mass, contractile force and time to exhaustion, radiating SR strands and compensatory hypertrophy of type II fibres, and interestingly a significant upregulation of SLN (*51*). These CNM features correspond most closely with the autosomal dominant form of CNM. Consistent with this, soleus muscles from the Pln^{OE} animals displayed increased Dnm2 levels, which is the genetically mutated protein in this form of human CNM. Murine models for this classification of CNM are lacking as the most common mutant variation, R465W Dnm2, display only impaired contractility and muscle atrophy with no central nuclei or type I fibre predominance (*71*). It is of importance to note that although there are no human cases of CNM associated with mutations in the gene for PLN, the Pln^{OE} model seems to more closely replicate

autosomal dominant CNM than any other mouse model to date. As well, biopsies from patients with varying forms of CNM have shown a trending increase in the expression of both monomer and total PLN compared to healthy counterparts (*51*). These findings, along with the sporadic cases of RYR1 mutations, suggest a link between Ca^{2+} dysregulation and the etiology of CNM which creates a new avenue to research potential therapeutic strategies as there is currently no treatment for CNM patients.

Calcium and Calcineurin in CNM

One of the most characteristic aspects of CNM is the localization of the cellular symptoms to type I fibres. In the Pln^{OE} model this phenomenon occurs due to the attachment of the PLN overexpression transgene to the MHCI promoter, however the clear mechanism that drives this phenomenon in human patients with CNM is yet to be uncovered. As can be seen in both the Pln^{OE} model of CNM and human Dnm2-CNM muscles, type I fibres progressively atrophy, while type II fibres either show compensatory hypertrophy due to an increased workload or transition to type I fibres becoming susceptible to the CNM related damage(*51, 61*). These fibre type transitions and corresponding progression of the severity, may be due to calcineurin (CnA), a serine-threonine phosphatase that is known to initiate a calcium-dependent signaling cascade leading to the promotion of type I or slow-twitch fibre gene expression (*72*). Increases in cytosolic Ca^{2+} activate CnA by creating a complex with calmodulin, which binds to the catalytic subunit of CnA and disrupts its autoinhibition (*73*). Once active, CnA dephosphorylates nuclear factor of activated T-cells (NFAT) proteins, which are a family of transcription factors containing five isoforms (NFATc1-4 and NFAT5) (*74*). Under normal physiological conditions, NFATs are heavily phosphorylated and located in the cytoplasm with expression in a variety of cell types. Upon desphosphorylation via CnA, a nuclear localization

signal is uncovered and NFATs translocate to the nucleus where they act as transcription factors (*75, 76*). Activated CnA and dephosphorylation of NFAT are part of a signaling pathway that has been shown to participate in a range of cellular adaptation processes, including immune cell activation (*76*), myoblast recruitment (*77*), myotube differentiation (*78*), and slow-twitch fibre type selection (*79*). With respect to fibre type selection, activated CnA alone has been shown to be sufficient to promote slow twitch fibre shift in transgenic mice (*80*). As well, McCullagh et al. (2004) demonstrated that overexpression of active NFATc1 stimulates the expression of MHCI and represses both MHCIIX and MHCIIB in rat muscle *in vivo* (*81*). Correspondingly, NFATc1 has also been linked to the expression of other slow-twitch fibre type characteristics including myoglobin, and troponin I, further linking this specific NFAT isoform with the oxidative, type I muscle fibre profile (*82, 83*).

Preliminary analyses conducted for this thesis and later published in *Brain and Behavior (84),* strove to assess whether the CnA-NFAT pathway was over-activated in the Pln^{OE} model of CNM. Western blotting for CnA content showed a significant increase in the expression of CnA within slow twitch muscle, such as soleus and gluteus minimus of 4-6 month old Pln^{OE} mice compared to wild type (WT) counterparts. Interestingly, this elevation in CnA content was not seen in the Pln^{OE} diaphragm muscles, which present with the reduced type I fibre predominance and the milder CNM phenotype at a cellular level. In accordance with this, a significant increase in nuclear NFAT content was found in Pln^{OE} gluteus minimus and a trending increase in Pln^{OE} soleus. Again there was no difference in nuclear NFAT levels in diaphragm between Pln^{OE} and WT animals. Together these data indicate the CnA-NFAT pathway is over activated in adult Pln^{OE} slow twitch muscles and presenting a possible therapeutic target in this model.

This thesis aimed to determine whether blocking the fibre type shift in Pln^{OE} muscles, via the administration of a well-known CnA inhibitor, cyclosporin A (CsA), would alleviate the disease phenotype and restore or retain muscle function in this model. Due to the progressive nature of this disease and cellular phenotype, we assessed the use of CsA as a potential therapeutic treatment in mice aged 4-6 months with fully developed CNM characteristics and developing, 4-6 week old mice with a milder phenotype. CsA has been previously researched as a method to alter fibre type profiles. A dose of 250nM CsA almost entirely attenuated the shift to slow MHC expression seen with spontaneous contraction in cultured rat myotubes along with an increase in fast MHC expression (*85*). As well, the same 50mg/kg body weight/day dosage of CsA as used in this thesis, has previously been shown to halt the shift towards type I fibres in plantaris muscles during hind limb overload of wild type mice (*86*). CsA does have alternative functions which could have deleterious or beneficial affects, including: binding to cyclophiin and preventing the opening of the mitochondrial permeability pore(*87*) as well as being commonly used as an immunosuppressant in humans(*88*).

Conceptually, within the Pln^{OE} model, reducing the amount of type I fibres via CsA administration, would lead to an improved phenotype not only because the CNM disease characteristics are predominantly localized in type I fibres but also because PLN overexpression occurs specifically within type I fibres in this model. Although fibre type specific genetic mutations do not occur in human CNM cases, it is possible that, if successful, this strategy may be useful in other animal models of CNM and human CNM where type I fibre predominance, atrophy and cololaization of CNM characteristics with type I fibres are also present.

Statement of the Problem

To date, there is no treatment option for patients with CNM. As the presence of atrophied type I fibres that predominantly display the other CNM disease characteristics is a feature shared by all classifications of CNM, it is imperative to examine the potential pathways which may drive this phenomenon. This thesis examined the effects of CsA administration and reduced CnA activity in Pln^{OE} mice as a potential therapeutic strategy to prevent type I fibre predominance and alleviate the CNM phenotype in this model. Developing (4-6 week old) and adult (4-6 month old) Pln^{OE} animals were used in this study to determine whether CsA treatment is more effective in halting the progression or in reversing the CNM phenotype associated with the Pln^{OE} model.

Objectives

The objectives for this thesis were as follows:

1. To examine whether CsA treatment could prevent or reverse type I fibre predominance in muscles from Pln^{OE} mice.
2. To examine whether CsA treatment can reduce the other markers of CNM in muscles from Pln^{OE} mice, including: centrally located nuclei, central aggregation of oxidative activity, and fibrosis.
3. To examine the effects of CsA treatment on SERCA activity and the SERCA regulatory proteins, PLN and SLN
4. To examine whether CsA treatment will increase strength and muscle function in Pln^{OE} mice.
5. To examine whether CsA is a viable treatment for both developing (4-6 week old) Pln^{OE} mice and adult (4-6 month old) Pln^{OE} mice.

Hypothesis

The hypotheses in relation to these objectives listed above:

1. CsA treatment would decrease CnA expression and activity, increasing phosphorylated NFAT and preventing the transition towards type I fibres seen in Pln^{OE} mice in both age groups.
2. Any decrease in type I fibres from CsA treatment would also reduce the other CNM features; including central nuclei, muscle atrophy and central aggregation of oxidative enzymes and activity, and fibrosis
3. In accordance with fibre type, PLN and SLN content would be reduced in CsA treated muscles compared to vehicle in both age groups. As a result, SERCA activity would also be increased in CsA treated solei.
4. CsA treatment would increase muscle function as seen by an increase in force and contraction and relaxation dynamics as a result of both the decrease in the CNM phenotype and the decrease in PLN and SLN.
5. CsA treatment would be more apt to prevent the formation of CNM in the younger age group than to reverse the damage and phenotype seen in the adult age group.

Methods

Transgenic Mice

Transgenic mice were originally generated by Song et al. (*50*). Briefly, the PLN coding and cDNA regions were ligated into the β-MHC promoter. This transgene was then injected into fertilized mouse eggs and transgenic mice overexpressing PLN in their type I muscle fibres were developed. These commercially available mice were then purchased (000067-MU, Mutant Mouse Regional Resource Centre, Columbia, MO) to generate a colony at the University of Waterloo. In maintenance of this colony, animals were bred male heterozygous for the Pln^{OE} transgene to female wild type as we found a severe phenotype in homozygous mice that posed problems for examining mechanisms and potential therapies. To assess genotype, littermate animals were ear notched and the DNA samples were digested using pureLink Genomic DNA mini kit (Invitrogen, Carslbad, CA) and amplified through a polymerase chain reaction (PCR) method to delineate whether an animal was wild type or PLN overexpressing. Further details on the genotypeing protocol used can be found in the appendix. All animals were caged with littermates and given food and water ad libitum. For the duration of the study animals were housed in an environmentally controlled room on a 12:12hr light-dark cycle. All experiments were reviewed and approved by the University of Waterloo Animal Care Committee in accordance with the Canadian Council on Animal Care. The below treatments and assessments were conducted on mice in two age groups: developing (4-6 weeks) and adult (4-6 months). Ages were chosen according to previously mentioned research done by Fajardo et al (2015) on the progression of fibre type shifts in Pln^{OE} mice (*51*).

Cyclosporin A

Cyclosporin A was dissolved in a 50% DMSO and saline solution as per its hydrophobic nature at a concentration of 2.5mg/ml. A vehicle solution of DMSO and saline was also prepared in the same volume. Drug and vehicle preparation were made the evening before injection and stored at -20°C. *Pln*^{OE} mice were injected subcutaneously with 25mg/kg body weight of CsA or the equivalent volume of the vehicle twice a day for two weeks. Mice were weighed daily to capture any changes in body weight over the course of injections both to determine drug or vehicle dosage and any potential drops in weight associated with stress. At the end of the two weeks, mice were sacrificed for dissection and tissue collection.

Whole Muscle Contractility

After cervical dislocation, intact solei from *Pln*^{OE} mice were dissected and placed in an oxygenated bath (95% O^2, 5% CO^2) with Tyrode solution containing 121mM $NaCl_2$, 5mM KCl, 24mM $NaHCO_3$, 1.8mM $CaCl_2$, 0.4mM NaH_2PO_4, 5.5mM glucose, 0.1mM EDTA, and 0.5mM $MgCl_2$, pH 7.3, which was maintained at 25°C. The muscles were mounted between two platinum electrodes and force was electrically induced from 1 to 100Hz using a biphasic stimulator (Model 710B, Aurora Scientific, Inc.) Once the stimulation protocol was complete the muscle was removed from the bath, de-tendonized and weighed to allow for normalization of data. Peak isometric force across all frequencies of stimulation, and maximal rates of contraction and relaxation were recorded, normalized to cross sectional area and analyzed on Excel.

Histological, Histochemical and Immunofluorescence Staining

Soleus muscles were excised and mounted in O.C.T. compound cooled in isopentane before freezing in liquid nitrogen. Samples were then cut into 10μm thick sections and mounted to Vectabonded slides in a -20°C cryostat (Thermo Electronic). Histological staining with Hematoxylin and Eosin (H&E) was conducted to assess central nuclei counts. Percent central nuclei values were calculated by dividing the total number of fibres displaying central nuclei by the total fibre number for the entire section. Van Gieson staining f was performed to assess intramuscular fibrosis. Once stained, full section images were converted to greyscale in order to set a threshold for background staining and then fibrosis was calculated with ImageJ. Histochemical staining included succinate dehydrogenase (SDH) to assess oxidative activity and localization. A brightfield Nikon microscope linked to a PixeLink digital camera was used to acquire images of the stained sections and ImageJ software was used to analyze the images. Immunofluorescent staining was done for fibre type and NFAT assessments. Fibre typing was done as previously described (*89*) to determine muscle fiber type using primary antibodies from Developmental Studies Hybridoma Bank against the differing myosin heavy chain (MHC) isoforms: MHCI (BA-F8), MHCIIa (SC-71) , MHCIIb (BF-F3) . An Axio Observer Z1 fluorescent microscope was used to capture images of the slides and ImageJ was used to determine fiber type distribution and cross sectional area. Immunoflourescent staining for NFAT was conducted as per the protocol in the appendix. Quantification of colocalization between the NFAT and DAPI channels were conducted on whole sections and background was removed as previously discussed for fibrosis. Quantification of colocalization was completed using the Colocalization Colourmap plugin for ImageJ.

Colocalization Colourmap uses the following equation:

$$nMDPx,y = \frac{(Ia - \overline{Ia})(Ib - \overline{Ib})}{(Ia_{max} - \overline{Ia})(Ib_{max} - \overline{Ib})}$$

where Ia and Ib denote the intensity of a given pixel in images a and b, $\overline{Ia}$ and $\overline{Ib}$ represent average intensities for their corresponding images and Ia_{max} and Ib_{max} are the highest pixel intensity in each image. This equation is used to assess the channel images from DAPI and NFAT staining and results in an index of correlation for two images, where a value of 0 corresponds with no colocalization and a value of one indicating full colocalization of the two channels.

Western Blotting

Western blotting was done for the following proteins: CnA, PLN, SLN, NFAT and Phospho-NFAT. Briefly, soleus sample was prepared with Laemeli buffer and loaded into SDS-polyacrylamide gels and ran electrophoretically for 75 min between 100 and 120V. Proteins were then transferred to a polyvinylidene difluoride (CnA, PLN, NFAT and p-NFAT) or a nitrocellulose (SLN) membrane on ice via wet transfer at 100V for 60mins (CnA, PLN, SLN) or for 45 minutes at 23V using semi-dry transfer methods (NFAT/p-NFAT). Membranes were then blocked in 5% milk in TBST (CnA, NFAT), signal enhancer (PLN) or BSA (p-NFAT, SLN) for one hour, after which primary antibodies were applied in varying concentrations in the corresponding blocking agent for one hour or overnight. Membranes were washed in TBST (3 times for 5 minutes) before and after an hour incubation in the corresponding HRP conjugated secondary antibody and Streptactin. After the final wash, chemiluminescence agents were applied to the membrane for detection and GeneTools (Syngene, MD, USA) was used to image and analyze the optical densities. A comprehensive list of details for all primary antibodies

information and dilution as well as protein load for each protein of interest can be found in the appendix.

Ca^{2+} ATPase activity

The Ca^{2+} ATPase assay as previously described by Duhamel et al. (2007) was done to assess SERCA activity in soleus homogenates of CsA and Veh treated Pln^{OE} mice (*90*). Ca^{2+} - dependent SERCA activity was measured at Ca^{2+} concentrations ranging from *p*Ca 7.0 to 4.5 using a plate reader assay on a spectrophotometer. GraphPad Prism was used to generate activity curves by non-linear regression curve fitting using a general sigmoidal model for substrate activity. SERCA activity was measured in the presence of Ca^{2+} ionophore A23187 (Sigma C7522) in order to reduce any back inhibition due to SR vesicle filling.

Statistical Analysis

All results are presented as means ± standard error of the mean (SEM). Unless otherwise stated, all statistical analyses were done using a two-way ANOVA to compare between treatment and age groups. Statistical significance was established at $p<0.05$. Graph Pad Prism Statistical Software was used for all statistical analyses and final image generation.

Results

Animal Physical Characteristics

Developing, 4-6 week old, and adult, 4-6 months old, *Pln*^{OE} animals were treated with either 25mg per kg body weight of CsA or the corresponding volume of vehicle (DMSO and saline) twice a day for two weeks. There was no significant difference between the change in body weight during injections between adult *Pln*^{OE} animals treated with CsA or vehicle. As expected, developing animals gained weight during the injection period, however similar to the adult groups there was no significant difference in delta body weight between CsA and vehicle treatments. Soleus to body weight ratios also did not change between animals treated with CsA or the corresponding dose of vehicle, regardless of age. However, there was a main effect of age for both delta body weight and soleus to body weight ratios meaning the 4-6 week old animals gained more body weight during injections and had larger soleus muscle for their size than the 4-6 month old animals, regardless of treatment.

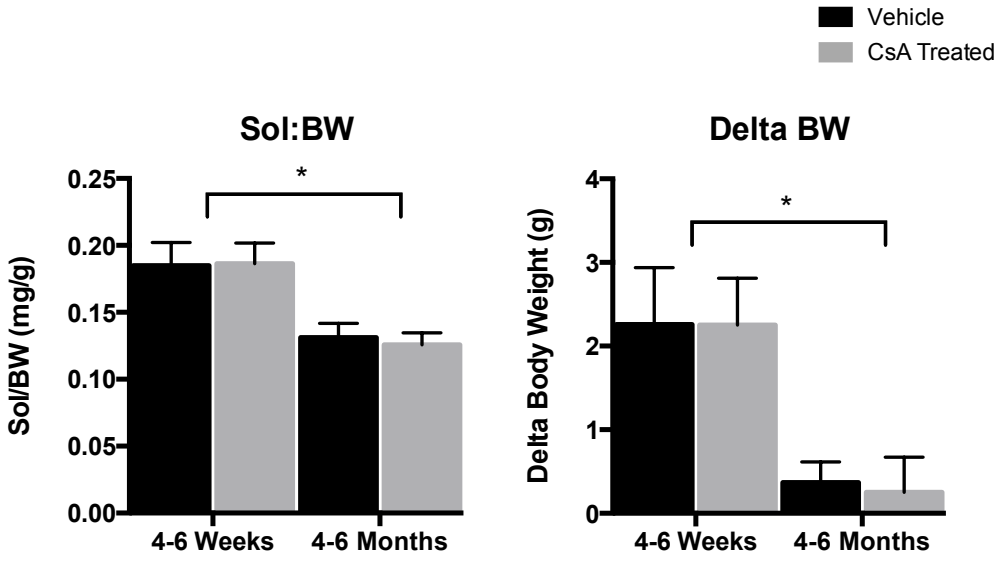

Figure 1. Delta Body Weight and Soleus: Body Weight of *Pln*^{OE} animals treated with CsA vs. Vehicle. Changes in body weight of *Pln*^{OE} animals post treatment with CsA or vehicle (A). Soleus weight (mg) normalized to total body weight (g) of CsA and vehicle treated *Pln*^{OE} animals (B). n=7 for 4-6 months and n= 3 for 4-6 weeks. * main effect of age. $P \leq 0.05$

Muscle Fibre Type and Cross Sectional Area

Fibre type distribution was assessed through immunofluorescence for MHC isoform (Fig. 3A) and analyzed using planned comparisons between treatments for each MHC isoform in both age groups. CsA treatment caused an approximate 10% reduction in the percentage of type I fibres in the soleus muscles from both 4-6 week old ($p=0.04$, Fig. 3B) and 4-6 month old ($p=0.03$, Fig. 3B) Pln^{OE} mice. In accordance with this, both age groups had a shift towards type IIA fibres, increases of 6% and 7% in developing animals ($p=0.04$, Fig.3A) and adult animals ($p=0.05$, Fig. 3A), respectively. However it is important to note that this treatment did not fully restore fibre type percentages back to wild type levels, which have been previously recorded at 45% type I and type IIA and 10% type IIB for wild type mice from this colony (*51*). Cross sectional area was assessed using a two way ANOVA to compare the effects of age and treatment on Pln^{OE} mice. There were no significant differences in the cross sectional area of type I fibres with CsA treatment in developing or adult mice (Fig. 3C). However, there was a significant main effect of age on the cross sectional area of type IIA fibres, with adult Pln^{OE} mice presenting larger type IIA fibres than the younger animals, regardless of treatment ($p=0.01$, Fig. 3C).

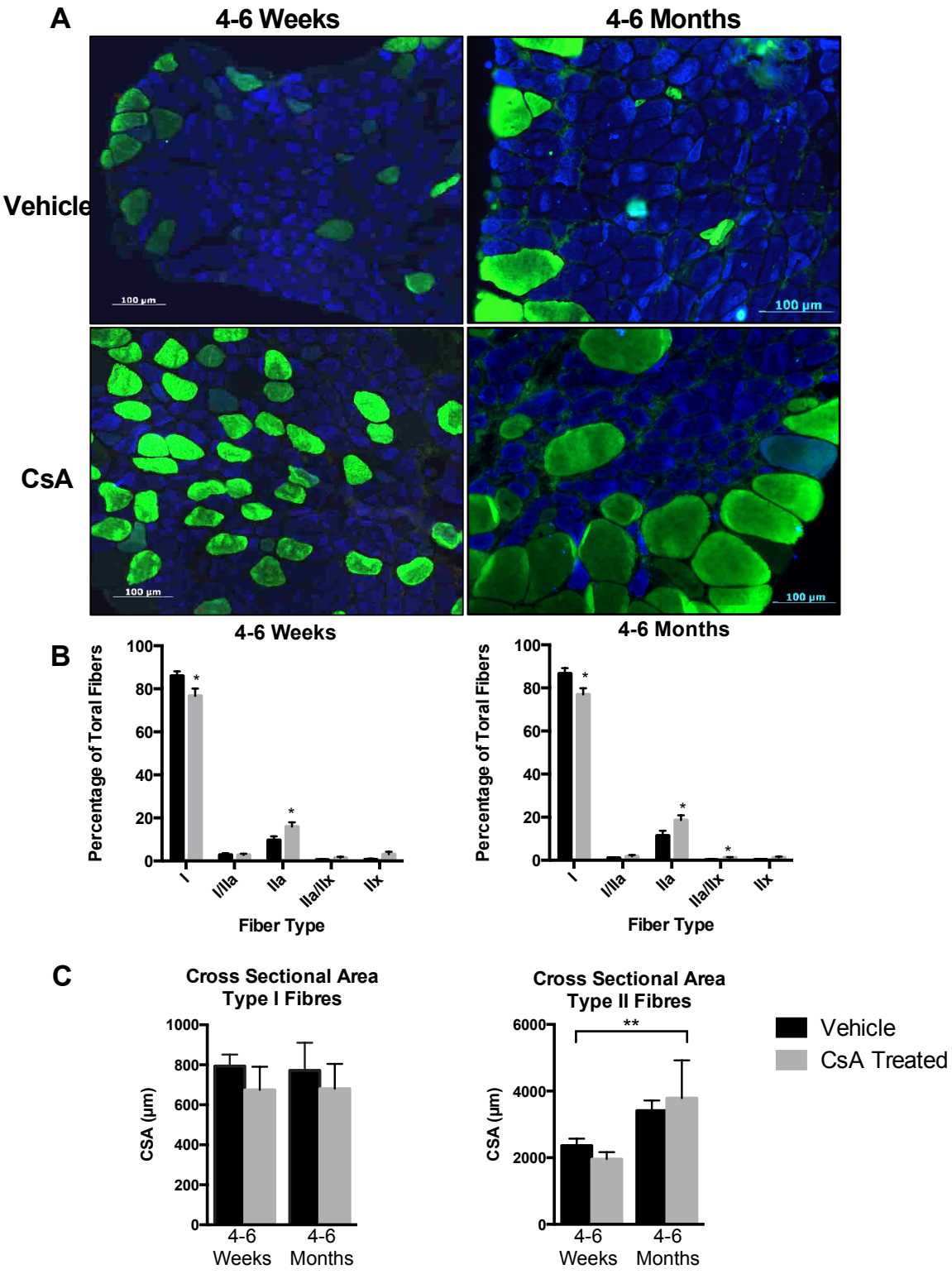

Figure 2. Fibre Type Changes in CsA treated *Pln*^{OE} soleus compared to Vehicle treated. Representative fibre type immunofluorescent images of soleus sections from 4-6 week and 4-6 month old animals treated with CsA or vehicle (A). Type I fibres are presented in blue and type IIa in green. Fibre type distributions (B) and cross sectional area (C) of individual fibre types were quantified from developing and adult *Pln*^{OE} mice treated with CsA or vehicle. n = 7 vs 6 for adult and n= 6 for developing. * significantly different from vehicle treated. ** main effect of age $P \leq 0.05$

Centronuclear Myopathy Features

It was hypothesized that blocking CnA activity and reducing the type I fibre predominance would result in a corresponding reduction in the presence of the other two disease features, namely abundant central nuclei and central aggregation of oxidative activity. However, although CsA treatment did decrease type I fibre predominance, there were no differences between CsA and vehicle in the presence of central nuclei across age groups. There was a main effect of age, with older 4-6 month animals displaying increased central nuclei regardless of treatment (p=0.02, Fig 3B).

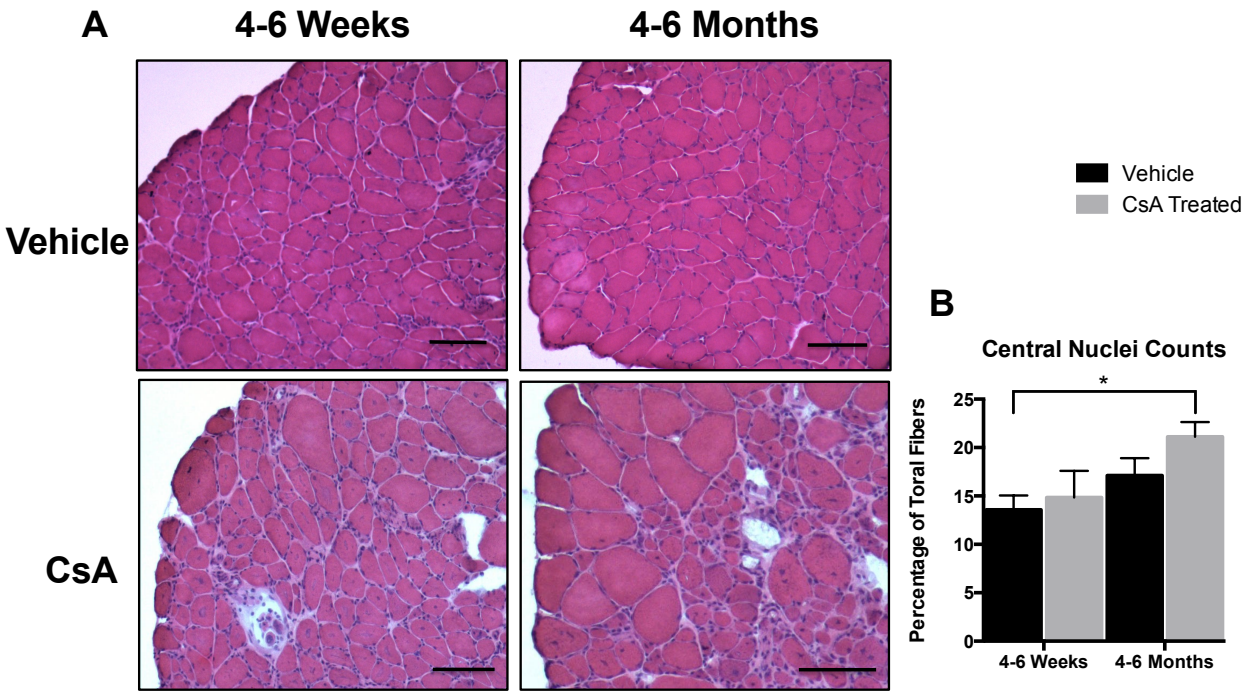

Figure 3. Central Nuclei Counts in *Pln*^{OE} soleus muscles treated with CsA or vehicle. Hematoxylin and Eosin staining was conducted on the soleus muscle of animals treated with CsA or vehicle at 4-6 weeks and 4-6 months of age (A). Quantification of total central nuclei counts was then done using Image J software (B). n=6 vs. 7 at both age groups. All scale bars are 100μm **main effect of age. P ≤ 0.05

As can be seen in Figure 4 and in accordance with central nuclei percentages, SDH staining revealed that the presence of dense bodies in the interior of the fibre persisted in CsA treated soleus muscle cross sections, denoting the central aggregation of oxidative activity. Although these dense, centrally located SDH staining persisted in both age groups, as of yet, there has been no successful way to quantify the presence of this phenomenon so it is unclear as to whether the occurrence of this CNM characteristic was altered with CsA treatment.

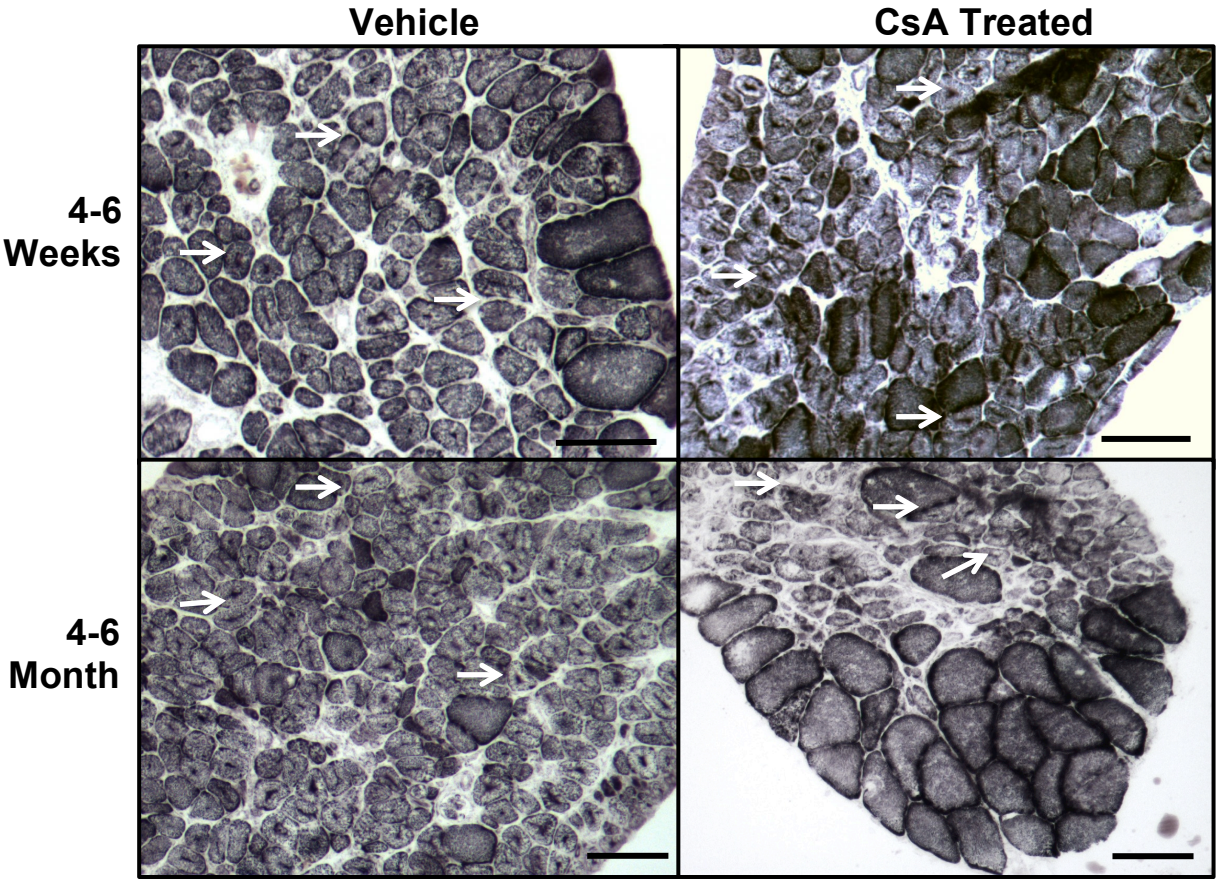

Figure 4. Abnormalities in SDH staining in *Pln*^{OE} animals regardless of treatment. Representative images of Succinate Dehydrogenase staining completed on soleus cross sections of *Pln*^{OE} animals treated with either CsA or vehicle at 4-6 weeks or 4-6 months of age. All scale bars are 100μm

Van Geison staining was done to assess the level of intracellular fibrosis in soleus muscles of *Pln*^{OE} animals treated with CsA and vehicle. A significant interaction effect was found, with younger 4-6 week old mice presenting less fibrosis than the adult 4-6 month old animals ($p<0.0001$, Fig. 5B) and CsA treated mice having significantly less fibrosis than their vehicle treated counterparts ($p=0.001$, Fig. B). Post hoc analysis also revealed a significant difference in the percentage of fibrosis between the 4-6 month old vehicle treated animals and all other groups.

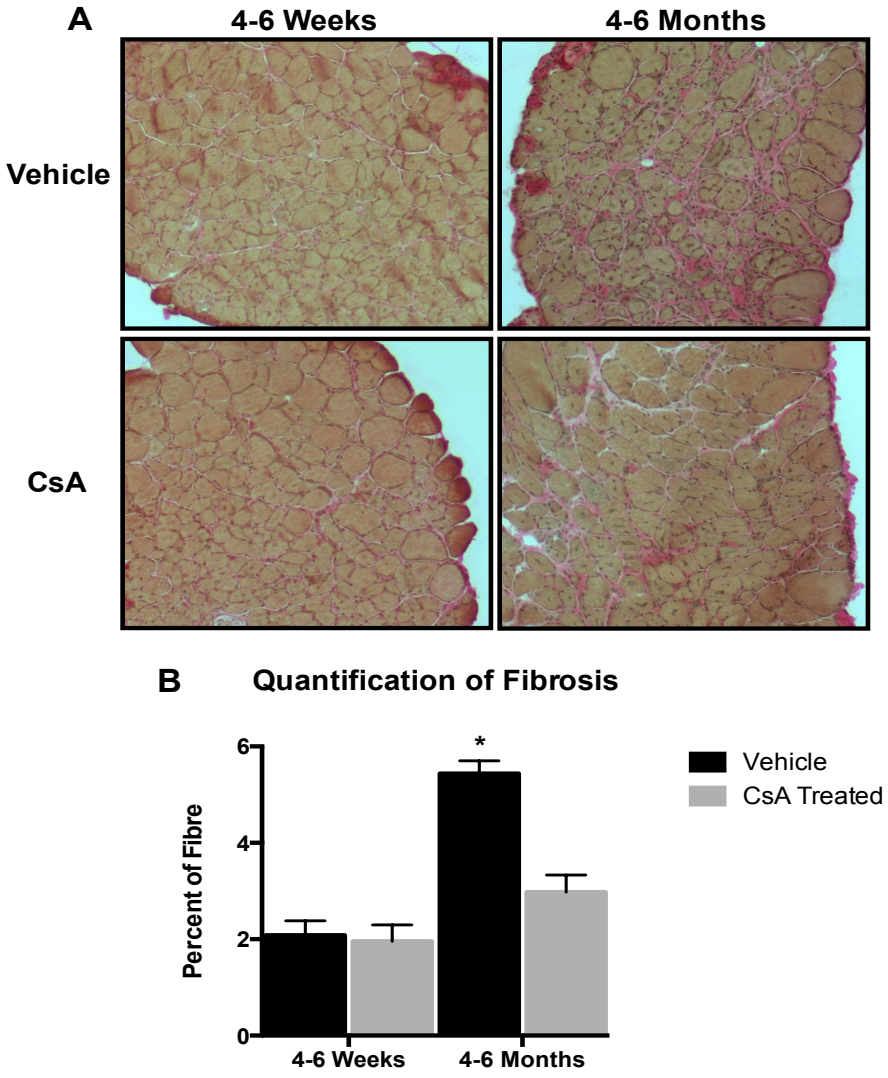

Figure 5. Effects of CsA and Vehicle treatment on Fibrosis of PLN^{OE} Soleus. Representative images of Van Geison staining between CsA treated and vehicle treated animals 4-6 weeks (n=4) and 4-6 months old (n=3) (A). Quantification of intracellular fibrosis (B). * significantly different from all other groups. A significant interaction effect between age and treatment was found for fibrosis. $P \leq 0.05$

Phospholamban and Sarcolipin

As expected, Western blotting showed a drop in the expression of PLN in the soleus of CsA treated animals compared to vehicle treated muscles at 4-6 months of age (p=0.03, Fig. 7E). As well, the same membrane was analyzed for pentamer PLN revealing a slight but non-significant increase in the inactive pentamer PLN in the CsA treated soleus compared to the vehicle treated muscle (p=0.32, Fig. 6F). When assessed in relation to one another, there was a significant reduction in the monomer to pentamer PLN ratio which indicates a reduction in the inhibitory function of PLN overall (0.03, Fig. 6G). In the younger, 4-6 week old Pln^{OE} mice treated with CsA there was no significant differences between monomer (p= 0.97, Fig. 6A) or pentamer PLN (p=0.30, Fig. 6B) and this corresponded with no change in the monomer to pentamer PLN ratio (p=0.60, Fig. 6C) between CsA and vehicle treated animals at this age. It should be noted, however, that there is still an overexpression of PLN in the treated animals at both age groups as monomer PLN in WT animals cannot be detected at this low protein load (2.5ug) (*51*).

As stated previously, there is a significant upregulation of SLN content in soleus muscles from Pln^{OE} mice, which could worsen the myopathy phenotype as SLN and PLN have been shown to cooperatively bind to SERCA causing super-inhibition of the pump. With CsA treatment there was a trending decrease in the SLN content in the soleus muscle of 4-6 month old animals compared to vehicle treated animals (p=0.10, Fig. 7H). As with nearly all the other findings thus far, no significant differences were found between SLN content with CsA treatment in the 4-6 week old animals (p= 0.18, Fig 6D).

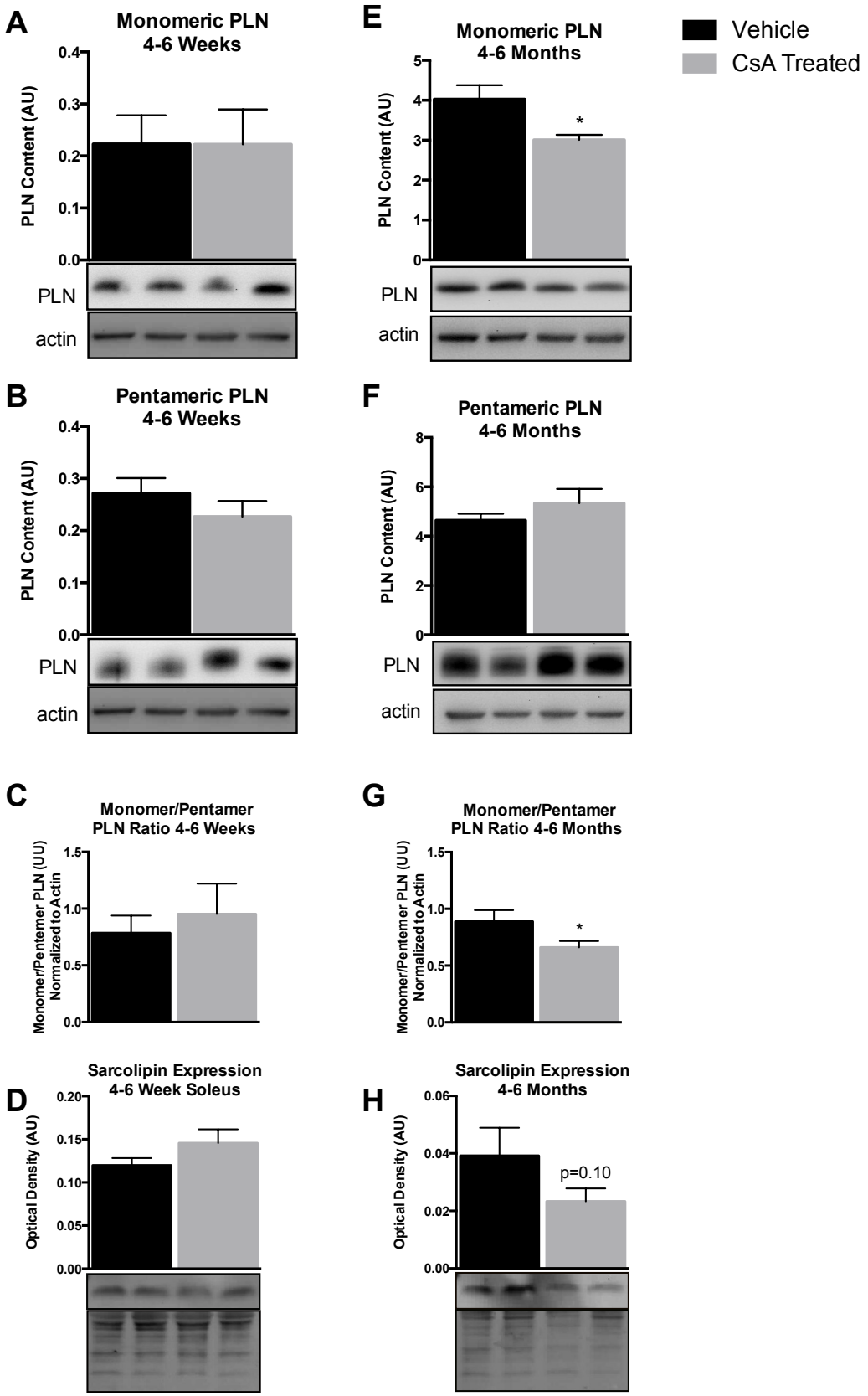

Figure 6. Phospholamban and Sarcolipin expression in CNM soleus treated with Vehicle or CsA. Western blotting for monomer (A&E) and pentamer (B&F) PLN and SLN (D&H) was conducted soleus homogenates of developing and adult *Pln*^{OE} mice treated with CsA or vehicle. Monomer to pentamer ratio was derived by dividing monomer density by pentamer density before normalizing (C&G). Optical densities were normalized to actin or ponceau depending on protein load. * significantly different than vehicle treated using standard student's t-test . n= 6 vs 7. P= 0.05

Whole Muscle Contractility

Whole soleus muscles were excised from CsA and vehicle treated Pln^{OE} mice and stimulated *ex-vivo*. Planned comparisons at each stimulation from 1-100Hz were done to assess muscle contractility between treatment groups. The solei of CsA-treated 4-6 month old Pln^{OE} mice displayed increased force per cross sectional area at all frequencies, with significance at twitch ($p=0.02$, Fig. 7E) and at the higher frequencies from 70Hz to 100Hz ($p<0.05$, Fig. 7E). This effect was not seen between the vehicle and CsA treated 4-6 week old animals (Fig. 7A). Maximal twitch and tetanic force for both vehicle and CsA treated developing and adult mice are shown in Figures 7B&F and 7C&G, respectively. Two way ANOVA analysis revealed no significant main effects for treatment or age for maximal twitch force, however there was a significant increase in twitch force per cross sectional area of CsA treated soleus versus vehicle treated of 4-6 month old animals ($p=0.05$, Fig. 7B). At maximal tetanic force there was a main effect of treatment, with CsA treated animals having increased force regardless of age ($p=0.05$, Fig. 7F). Although there was not an interaction effect between age and treatment, planned comparison analyses showed a significant increase in the maximal tetanic force of 4-6 month old CsA treated animals compared to all other groups ($p\leq0.02$, Fig. 7F).

Interestingly, there was no difference in rate of relaxation between vehicle and CsA treated solei during twitch stimulus for either age group (Fig 7C). However, when stimulated at 100Hz creating a tetanic contraction, there was a main effect of age with the solei of 4-6 month old animals relaxing slower in both treatment groups ($p=0.03$, Fig. 7G). Similarly, treatment had no significant effect on the rate of contraction at any age but there was a significant decrease in the rate of contraction in 4-6 month old animals compared to 4-6 week old animals across treatment groups ($p=0.02$, Fig. 7H).

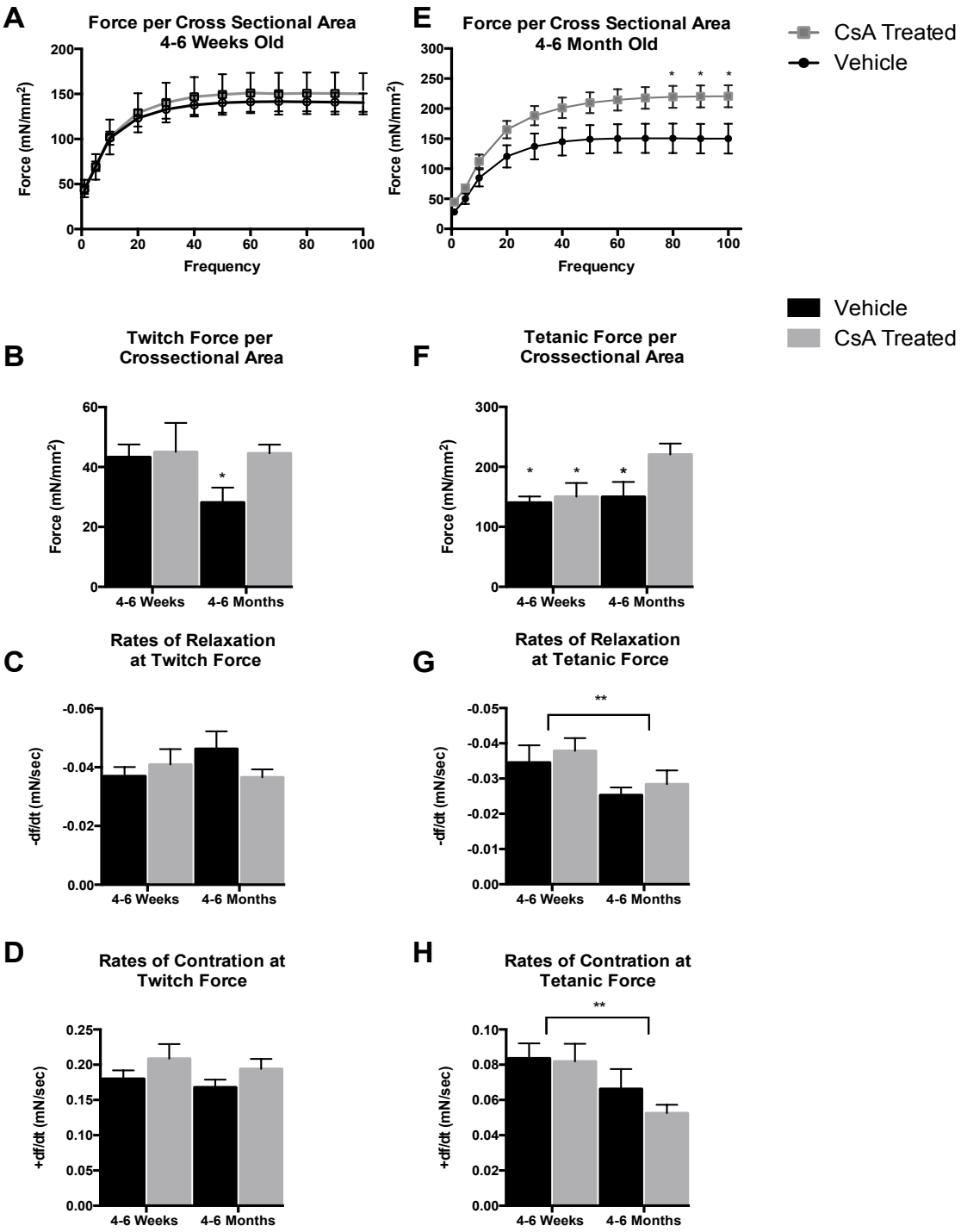

Figure 7. Force Analysis between CsA-treated and Vehicle *Pln*^{OE} animals at 4-6 Months and 4-6 Weeks. Force per cross sectional area frequency curve for soleus muscles from *Pln*^{OE} animals aged 4-6 weeks (A) and 4-6 months (E). Single twitch force (B) and 100Hz tetanic force (F) per cross sectional area for *Pln*^{OE} mice. Rates of relaxation between CsA and vehicle treated developing and adult *Pln*^{OE} animals for twitch (C) and 100Hz tetanic (G) contractions. * significantly different from adult CsA treated. ** main effect of age. n =6 vs 7. $P \leq 0.05$

Ca^{2+} ATPase Activity

As all of the previous data have shown CsA administration only improves the CNM phenotype and muscle function of adult, 4-6 month old Pln^{OE} animals, SERCA activity was assessed in the soleus muscles of the adult CsA treated animals and their vehicle treated counterparts. Surprisingly, there was no significant difference in the maximal SERCA activity (*V*max) (p=0.94), or the *K*Ca (p=0.98), denoting the pCa required to elicit half maximal SERCA activity, in CsA verses vehicle treated soleus muscle (Fig. 8).

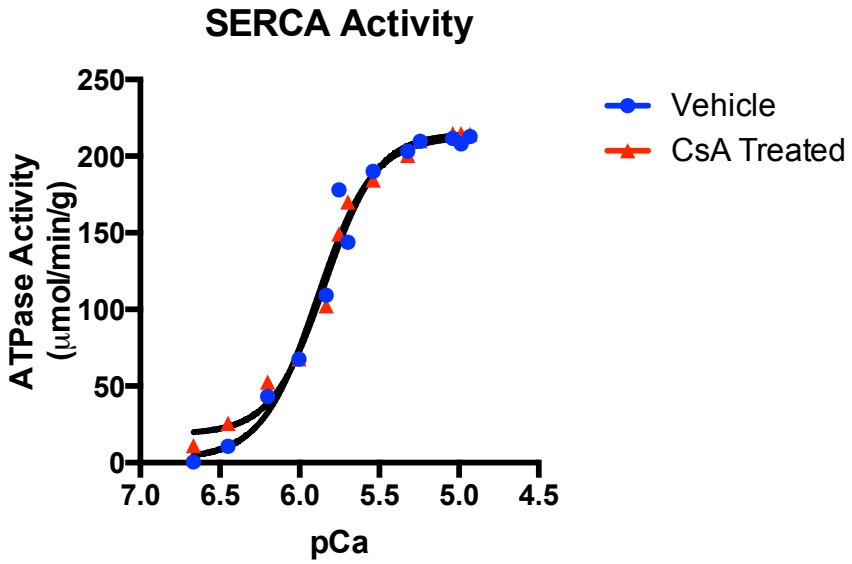

	*V*max	*K*Ca
VEH	220.3 ± 52.57	5.78
CSA	226.0 ± 52.08	5.79

Figure 8. SERCA Activity in the soleus muscle of 4-6 Month Old Pln^{OE} mice Treated with CsA or Vehicle. Ca^{2+}-ATPase activity -*p*Ca curves for soleus homogenates from CsA (n=3) and vehicle (n=4) treated Pln^{OE} mice. Values for *V*max and *K*Ca are listed as mean ± standard error of means. * significantly different from vehicle treated using standard student's t-test. $P \leq 0.05$

Calcineurin and NFAT expression

After administration of CsA for two weeks, there was a significant decrease in the expression of CnA within the soleus muscles of adult mice compared to their vehicle treated littermate counterparts ($p=0.05$, Fig. 9A). However, Western blotting showed no change in total NFATc1 content ($p=0.83$, Fig. 9B) but a significant reduction in phosphorylated NFATc1 ($p=0.04$, Fig. 9C) in treated soleus muscles compared to vehicle treated animals. When comparing NFAT-p to total NFAT, which should indicate the localization of NFAT, there was a significant decrease in the ratio of CsA treated soleus compared to vehicle treated suggesting increased nuclear localization of NFAT with treatment ($p=0.01$, Fig. 9D). This is in direct contradiction to the fibre type assessment and PLN content previously shown which would suggest lower CnA activity and reduced NFAT translocation to the nucleus.

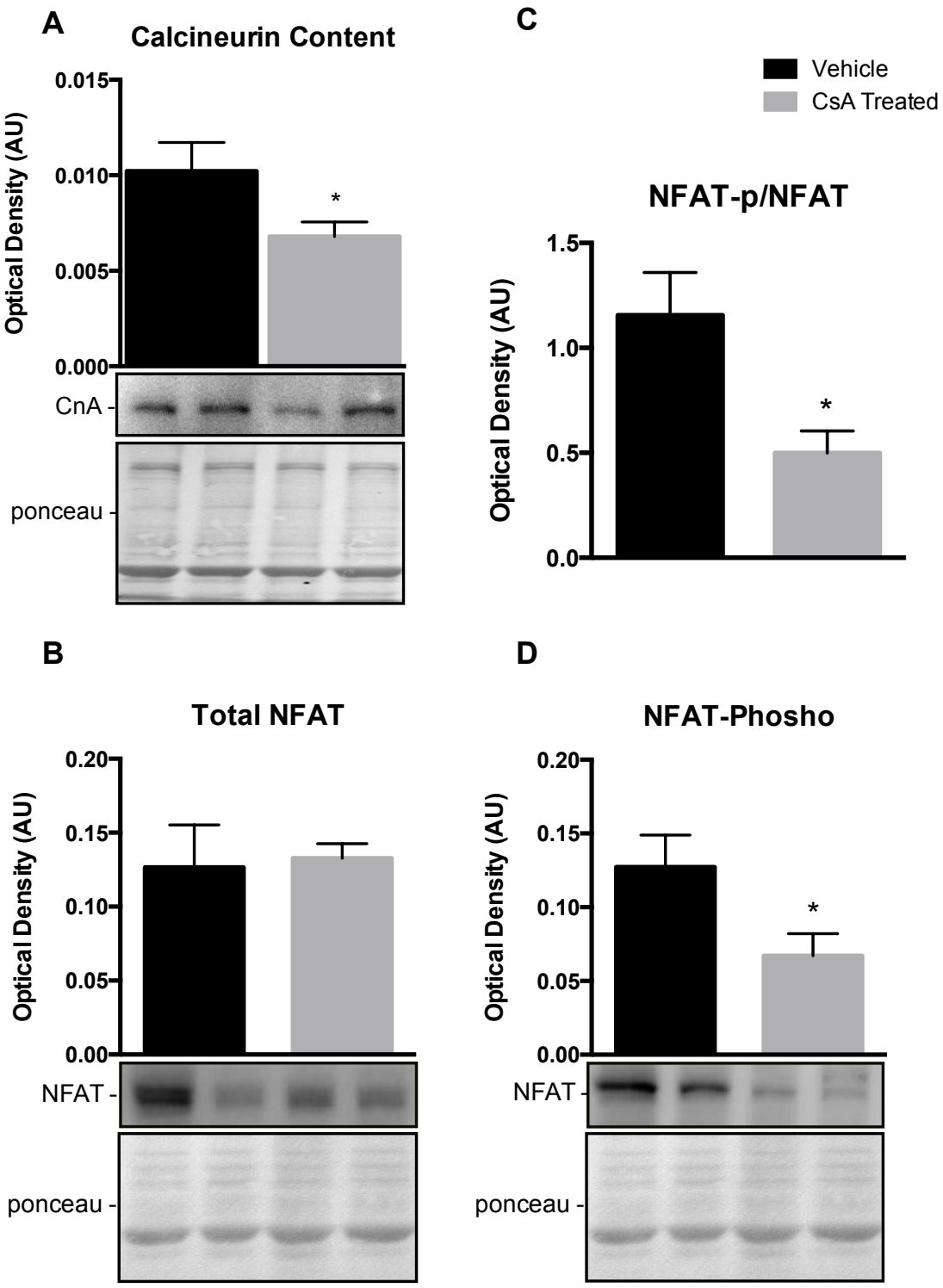

Figure 9. Calcineurin Content and NFAT localization in CsA and vehicle treated *Pln*^{OE} animals. Western blotting for CnA (A), NFAT (B), and NFAT-p (D) content in soleus samples from CsA or vehicle treated *Pln*^{OE} animals aged 4-6 months. NFAT-p content in relation to total NFAT content (C). All blots were normalized to total protein via ponceau stain. n=6 vs 7. * significantly different from vehicle treated using standard student's t-test. $P \leq 0.05$

In an attempt to clarify this discrepancy, immunofluorescence for NFATc1, along with DAPI and dystrophin for nuclei and the plasma membrane respectively, was conducted on serial cross-sections of soleus muscles from CsA and vehicle treated animals at both age groups. To quantify the colocalization of DAPI and NFAT, the statistical model adapted by Jaskoski et al. (*91*) was used. This model computes the correlation between a single pixel on two different channel images while maintaining the x and y coordinates which results in a correlation index where zero is equivalent to no correlation and one corresponds with total overlap of the two fluorescent signals of interest. Using this method, there was a significant main effect of treatment, with CsA treated animals displaying a significant decrease in the colocalization of NFAT and DAPI fluorescence compared to vehicle counterparts across age groups ($p=0.03$, Fig. 10C). Although there was not an interaction effect between age and treatment, planned comparisons show vehicle treated 4-6 month old animals showed significantly more NFAT and DAPI colocalization than all other groups including: their age matched CsA treated littermates ($p=0.03$) as well as both CsA ($p=0.01$) and vehicle treated ($p=0.04$) developing animals (Fig. 10C). These data corroborate with the fibre type shift and the reduction in the expression of PLN in adult but not developing Pln^{OE} mice, to suggest CsA administration decreased CnA activity and nuclear NFAT content in 4-6 month old animals and caused no difference in 4-6 week old animals.

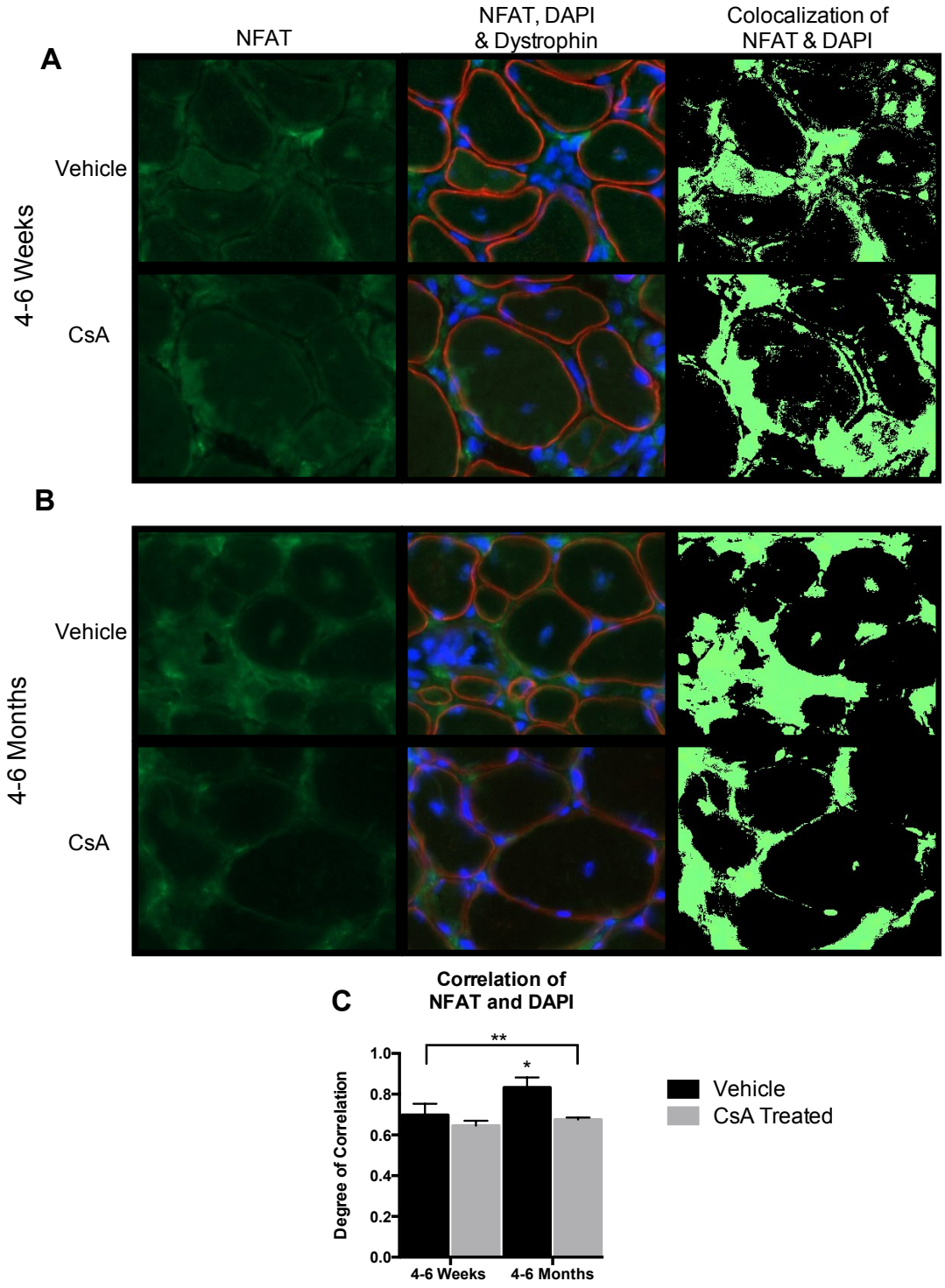

Figure 10. NFAT colocalization with Nuclei in CNM Soleus Treated with CsA or Vehicle. Representative images of immunofluorescence for NFAT (green), DAPI (blue) and Dystophin (red) along with colocalization images of NFAT and DAPI from CsA and vehicle treated Pln^{OE} mice aged 4-6 weeks (A) and 4-6 months (B)**.** Quantification of the colocalization of NFAT and DAPI. * significantly different from all other groups. ** main effect of treatment. $P \leq 0.05$

Discussion

The primary goal of this research was to examine whether pharmacological inhibition of CnA using CsA is an effective therapeutic strategy to alleviate CNM and improve skeletal muscle function in *Pln*^{OE} mice. As hypothesized, a two-week dosage of 50mg/kg body weight/day of CsA administered to *Pln*^{OE} mice resulted in a significant reduction in the predominance of type I fibres and increased hybrid and type IIA fibres in both 4-6 week and 4-6 month old age groups. These fibre type transitions suggest that CsA treatment was successful in blocking the dephosphorylation of NFAT by CnA and the promotion of MHCI transcription. However, this is a modest reduction as the CsA treated *Pln*^{OE} solei were still 35% above what is expected of a wild type animal of this background (*51*). With the exception of one other study by Michel et al. (2007), who reported that the same dosage of CsA completely prevented the shift towards type I fibres in surgically overloaded plantaris muscles from CD-1 male mice (*92*), there is no other study in the literature to compare our results with. The effects of CsA on muscle fibre type observed in this study are not even really comparable with the study by Michel et al., as the models examined are very different.

Unexpectedly, there were no significant differences in the cross sectional area of specific fibre types between treatment groups in this study. There is contradictory evidence as to whether CnA activity is essential for the promotion of muscle hypertrophy either through activating the Akt/mTOR pathway, regulating myostatin expression, or interacting with MEF2 (*93, 94*). Michel et al. have suggested that hypertrophy is blunted with high dosages of CsA such as the one used in this study. However, 4-6 month old *Pln*^{OE} mice had significantly larger type IIA fibres across treatment groups, which could suggest hypertrophy was not blocked during the CsA treatment or that previous compensatory hypertrophy was maintained during treatment. Additionally in this

study, any potential increase in the cross sectional area of type II fibres may be masked by the variance introduced as smaller atrophied type I fibres transition towards type II.

One possible explanation for the fairly modest effects of CsA treatment on muscle fibre type and size in Pln^{OE} mice could also be a low treatment efficacy and less inhibition of CnA than expected. In this regard, the results are mixed for measures of CnA activity and for the different age groups examined in this study. In adult 4-6 month old animals, immunofluorescence analyses show that CsA treatment resulted in a decrease in the colocalization of NFATc1 and DAPI fluorescence, indicating that CsA treatment was successful in blocking the CnA- dependent dephosphorylation of NFAT, resulting in less shuttling of NFAT into the nucleus. As well, CnA content was reduced in CsA treated adult animals compared to vehicle treated littermates, suggesting reduced CnA activity. However, in direct contrast to the immunofluorescence data, Western blotting analyses indicated a reduction in phosphorylated NFATc1 with no changes in total NFATc1 in response to CsA treatment. Those results imply that CsA treatment actually increased CnA activity resulting in increased nuclear NFAT. However, that is very unlikely since increased CnA signaling would be expected to promote type I fibre gene expression and here, the percentage of fibres expressing MHCI was reduced following CsA treatment which corresponds better with the immunofluorescence data showing reduced nuclear NFAT, at least in 4-6 month old mice. Further complicating the interpretation of these results is the fact that CsA treatment in 4-6 week old animals resulted in decreased type I fibre percentage but CnA signaling as indicated by immunofluorescence analysis of nuclear NFAT, was not different compared with vehicle. Taken together, the results suggest that CsA treatment was successful at blunting CnA activity in the soleus, and probably more so in 4-6

month old animals than 4-6 week old animals, but this conclusion is less convincing given the discrepancy in results noted above.

There are several factors that could contribute to the discrepancy in the measures of CnA signaling such as the role of other NFAT isoforms and the phosphorylation and nuclear export of NFAT. As mentioned previously, there are five members of the NFAT protein family. NFATc1-4 are activated through the Ca^{2+}/calcineurin pathway while NFAT5, the primordial isoform, is activated by osmotic stress (*95*). Although there is some redundancy in function, the four Ca^{2+} -dependent isoforms have been linked to differing downstream consequences. NFATc1 deletion substantially reduces cytokine production suggesting its importance in the innate immune response (*96*). A developmental role for NFATc2 is presumed due to impaired myoblast fusion and regeneration post injury in NFATc2 null mice (*78*). NFATc3 has been found active in a transgenic mouse model of Parkinson's disease with increased cytosolic [Ca^{2+}] in midbrain dopaminergic neurons (*97*). Deletion of two or more NFAT isoforms also has differing effects on phenotype. For instance, deletion of NFATc1 and NFATc2 results in effective loss of cytokine production in T-cells while deletion of NFATc3 and NFATc4 promotes defects in vascular developmental organization and results in embryonic death (*98*). This heterogeneity between specific NFAT isoforms is also present within skeletal muscle. Abbott et al. (1998) showed a clear pattern of expression during differentiation of cultured human skeletal muscle cells, with NFATc1, NFATc2, NFATc3 corresponding with myoblasts, nascent myotubes and mature myotubes, respectively (*99*). Correspondingly, differences in mice lacking specific NFAT isoforms have been witnessed such that mice lacking NFATc3 have a reduction in myofibre number while NFATc2 null mice show impaired muscular hypertrophy (*78, 100*). In respect to fibre type promotion, the NFAT-MHC isoform patterns are complex as well. Promotion of

neonatal MHC has been linked solely to NFATc2 while NFATc1 and NFATc3 preferentially bind to the promoter for embryonic MHC (*101*) Historically the expression of MHCI has been associated with NFATc1. Indeed, a constitutively active NFATc1 mutant stimulated the MHCI transcription while inhibiting the fast MHCIIb promoter (*81*). As well, a transgenic mouse line with skeletal muscle specific knockout of NFATc1, has shown decreased percentages of type I fibres compared to wild type littermate (*102*). In this thesis, assessment of NFATc1 was chosen because of its strong association with MHCI expression in the literature. However, Calabria et al. (2009) has demonstrated that this may not be such an exclusive relationship by inducing a knockdown of individual NFAT isoforms 1-4 and assessing the corresponding effect on DNA promoters for the differing adult MHC isoform (*103*). In their study, the MHCI promoter was blunted in all the NFAT isoform knockdowns, which indicates that the transcriptional regulation of MHCI by each isoform may not be redundant. This is an imperative piece of data for this thesis as NFATc1 may not be the sole isoform driving MHCI expression. Further assessment should be done on additional NFAT isoforms to confirm localization in order to truly show the link between the CsA treatment and the downstream fibre type variations.

The rate at which NFAT is shuttled in and out of the nucleus is also necessary to consider for the understanding of the discrepancies in our data. As discussed previously, dephosphorylaton and nuclear import of NFAT isoforms occurs via CnA activation and has been reported to occur as quickly as 15 minutes after a sustained Ca^{2+} signal (*104*). Nuclear export of NFAT is also highly regulated and achieved by the phosphorylation and subsequent covering of nuclear localization signal. NFAT export can be achieved through several kinases, including glycogen synthase-3 kinase (GS3K) (*105*), casein kinase 1 (CK1) (*106*), protein kinase A (PKA) (*107*), MAP kinases p38 and JNK*(108)*. As NFAT isoforms have upwards of 18 phosphorylation

sites dispersed throughout the regulatory region, the coordination and combination of these kinases is required for inactivation and nuclear export. The timing for nuclear export varies between different cells/tissues with rapid export in lymphocytes and prolonged nuclear localization of up to two hours in neurons (*109, 110*). The timing of both import and export have yet to be uncovered within skeletal muscle but are important to consider when interpreting the findings of this study. As sample preparation varies for Western blotting and immunofluorescence, a rapid shift in localization of NFAT from cytosol to nucleus and back may explain the differing results for NFAT localization with CsA treatment in Pln^{OE} mice.

Interestingly, the modest reduction in type I fibre predominance corresponded with a significant reduction in both monomer PLN and the ratio of monomer to pentamer PLN in the 4-6 month old mice, further supporting the view that the CsA treatment was successful in blocking transcription of MHCI and the attached transgene for PLN in those mice. The decrease in monomer PLN content would be expected to correspond with an increase in SERCA activity due to less inhibition of SERCA by active, monomer PLN. PLN has previously been shown to regulate rates of relaxation, with PLN ablation showing a marked increase in the rate (*41*) and overexpression of PLN causing greatly reduced rates of relaxation (*50*), As such, it was also hypothesized that rates of relaxation would be increased due to the reduction in monomer PLN, however there were no significant differences in rates of relaxation between treatment groups. Surprisingly. but consistent with the lack of difference in relaxation rates between groups, there were also no differences in SERCA activity between CsA and vehicle treated animals. The discrepancy between the reduction in PLN and its effect on SERCA activity and relaxation are surprising; however, PLN has been previously shown to dissociate from SERCA with high intracellular Ca^{2+} (*111*). As such, speculation on the inhibitory effects of PLN on SERCA activity

during the contraction-relaxation cycle cannot occur without further research into the co-immunoprecipitation of SERCA and PLN in this model.

With respect to other histological and functional markers of CNM, there was also a decrease in the presence of intracellular fibrosis indicating a milder CNM phenotype following CsA treatment, but only in 4-6 month old animals. Although it t is unclear as to whether this reduction in fibrosis is attributable to a generally improved phenotype or to the specific inhibition of CnA, as it has been shown to activate fibroblasts and collagen synthesis in cardiac muscle (91), it did corresponds with improved muscle function. Compared with vehicle, CsA treatment produced an improvement in soleus force per cross sectional area at both twitch and tetanic frequencies at 4-6 months of age. In light of these findings, it seems CsA was successful in moderately improving both fibre type and muscle function within this model of CNM for animals aged 4-6 months.

However, treatment with CsA did not affect the percentage of centrally located nuclei as was hypothesized. There was a main effect of age, with older 4-6 month animals displaying increased central nuclei across treatment groups. Although central nuclei are considered a negative disease characteristic in CNM, satellite cell proliferation and differentiation to regenerate myo-neuclei is also well documented within myopathies and injury wherein central nuclei are present (*112*). Future assessments into the colocalization of Pax7, a satellite cell marker, with centrally located nuclei should be done to determine whether there are more regenerating fibres with CsA treatment than vehicle treated animals.

Corresponding with central nuclei, the persistence of dense SDH staining in the interior of the fibre was also observed in CsA treated animals. Unequal SDH staining between fibres is

also related to the muscle fibre type, with the darkest staining found in type IIA fibres, which are the most oxidative rodent fibre. As can be seen in Figure 5, a noticeable correlation exists between fibres with lighter SDH staining, corresponding with type I fibres, and the presence of central aggregation of SDH bodies. Previous studies have linked this abnormal SDH staining with significant decreases in cytochrome c oxidase activity and ATP levels in primary muscle cells from 4 X-linked CNM patients and in MTM1 KO mice (93). The persistence of this CNM feature in both age groups indicates that CsA was unsuccessful in reducing this abnormality.

Together, both the central nuclei and SDH findings suggest that the origin of these CNM characteristics is not associated with the transcription of MHCI. Several cytoskeleton proteins have been uncovered in connection to cellular development and organelle organization but the mechanisms by which organelles, such as nuclei and mitochondria, navigate to their proper position is not fully understood. One such associated protein is DNM2. Both mice and humans with X-linked CNM show an upregulation of DNM2 and treatment to reduce DNM2 has been shown to improve intracellular organization within these tissues (*113*). The Pln^{OE} CNM model also displays an overexpression of DNM2, which may be more responsible for the improper localization of nuclei and mitochondria than the CnA-NFAT pathway. As well, there is evidence to suggest that these histological features do not directly determine the severity of the disease as seen in the Chen et al (2014) review of DNM2-CNM where a patient with the highest central nuclei counts (93%) maintained the ability to self-ambulate much longer than other patients with lower central nuclei counts (*114*). This corresponds with the findings of this thesis in that there were CsA treatment improvements in muscle contractility with no changes in some CNM features, namely central nuclei and central oxidative activity.

There was also nearly a 50% reduction in the expression of SLN in CsA treated verses vehicle treated 4-6 month old animals although this finding was statistically non-significant (p=0.1). Nevertheless, this is an interesting finding as there is evidence to suggest it may have a positive or negative effect on phenotype. As mentioned previously, SLN and PLN together can bind to SERCA and cause super inhibition of the pump. As such, the findings in this thesis showing a reduction in both PLN and SLN should partially relieve this inhibition and alleviate some of the detrimental effects of chronically elevated Ca^{2+} thought to be involved in this CNM model. Conversely, unpublished data from our lab have shown that when SLN is ablated in this mouse model it worsens the myopathy, with SLN knockout-Pln^{OE} (SKOPOE) animals exhibiting increased muscle atrophy, weakness, and a reduction in total muscle fibre count (*115*). Interestingly, the soleus muscles of these SKOPOE animals also presented reduced CnA activity and an inability for compensatory type II fibre hypertrophy. From the two models, Pln^{OE} and SKOPOE, it can be seen that a bivariate relationship exists between CnA activity and SLN expression, in that CnA activity may regulate SLN expression and hypertrophy and SLN expression may be required for CnA activity and hypertrophy. Therefore the reduction in SLN witnessed with CsA treatment may be a result of reduced CnA activity. Whether this SLN reduction is detrimental to phenotype as with the SKOPOE mice or if it is a beneficial effect of CsA treatment in Pln^{OE} mice that partly contributes to an improved overall muscle health and function is yet to be determined from this research.

Finally, it was originally hypothesized this CsA treatment would be more effective in the younger, 4-6 week old animals as it would be more effective to block CnA activity before the full CNM phenotype was achieved. The results of this study do not support this hypothesis. Although the same CsA dose did significantly blunt the development of type I fibre type

predominance, many of the other improvements, such as improved force and decreased fibrosis were not evident in the younger animals. As reported by Fajardo et al. (2015), the CNM phenotype within this model is progressive reaching a severity plateau at 4-6 months of age (*51*). Many findings in this thesis correspond with this progression, including increased soleus to body weight ratios, increased twitch force, decreased fibrosis and decreased central nuclei counts in comparison to vehicle treated older animals. There was also a significantly lower colocalization of DAPI and NFAT in the both CsA and vehicle treated 4-6 week old animals compared to vehicle treated 4-6 month old mice, which suggests that the CnA-NFAT pathway is less activated at the younger age. Furthermore, as mentioned above, treatment efficacy may have been lower in the 4-6 week old animals since immunofluorescence measures of CnA signaling did not reveal any evidence that CsA blocked CnA activity at that age. Taken together the improvement of the myopathy may have been harder to detect with the milder CNM phenotype and reduced activation of CnA associated with 4-6 week old animals. Future studies may pursue administering a longer CsA treatment protocol and increasing the power of the assessment by adding additional animals or assessing the optimal age for treatment.

NFAT proteins show activation, dephosphorylation and nuclear import, with low sustained Ca^{2+} plateaus but seem to be insensitive to more rapid, larger influxes of Ca^{2+} (*116*). Interestingly, this is a similar activation pattern seen with PLN, wherein PLN is bound to SERCA at chronic, low Ca^{2+} levels and disassociates from the pump upon higher Ca^{2+} transients. Theoretically these findings would suggest that in a model with such prolific PLN overexpression, CnA activation may be attributable to PLNs interaction with SERCA as the delay in uptake of Ca^{2+} into the SR could be sufficient to initiate the formation of the Ca^{2+}-calmodulin complex. That being said, one of the major limitations in this study and previous

research done using this Pln^{OE} mouse model for CNM is the lack of a direct measure of intracellular Ca^{2+} concentrations. It is assumed the overexpression of PLN, and corresponding inhibition of SERCA, has increased intracellular [Ca^{2+}] but we and others have not directly measured cytosolic Ca^{2+} in intact muscles. Although difficult to do, measurement of intracellular [Ca^{2+}] *in vivo* is possible. Intracellular Ca^{2+} has been quantified using the Ca^{2+}-fluorescent dye, Indo-1, to assess both resting Ca^{2+} levels and Ca^{2+} dynamics during depolarization of enzymatically isolated single muscle fibres from $mdx^{-/-}$ animals (*117*). That being said the dystrophic phenotype witnessed in $mdx^{-/-}$ mice presents a less severe myopathy than the Pln^{OE} model of CNM and the single fibre dissections may prove to be problematic. Success in quantifying intracellular Ca^{2+} would help to define whether Ca^{2+} dysregulation is responsible for the CNM phenotype and, if so, it would help gauge the ability of treatments in targeting Ca^{2+} and its associated pathways.

Finally, although extensively discussed in relation to fibre type in this thesis, CnA and NFAT are also responsible for activation of the innate immune response. Congruent with this, CsA treatment is widely used in immunosuppression in humans and has been shown to reduce the activation of many diverse immune cell types (*76, 118-121*). Therefore, treatment of Pln^{OE} animals with the relatively high dose of CsA used in this study would effectively suppress any immune system response. This immunosuppression should be noted with respect to the side effects it would cause for patients. This thesis may give merit to the concept of fibre type targeting as a potential treatment strategy, however the immune suppression associated with CsA treatment is substantial and may limit its clinical use for treatment of CNM in humans.

Future Directions and Conclusion

Moving forward, I believe there are still many potential avenues to target PLN as a therapeutic target for CNM; however, it is first necessary to truly uncover the connection between this SERCA-regulatory protein and CNM. Two main theories present themselves when trying to uncover the mechanism in which the overexpression of PLN causes CNM. The first is tied to the regulatory role of PLN and its effects on Ca^{2+} levels. In theory, the overexpression of PLN, and the subsequent reduction in SERCA activity, would result in high intracellular [Ca^{2+}]. This elevated cytosolic [Ca^{2+}], has been linked to several detrimental downstream effects such as central nuclei, increased protein degradation, calpain activation, and mitochondrial swelling and rupture (*29, 122, 123*). Several features of this CNM model support this theory, including increased calpain activity, the predominance of MHCI and irregularities in SDH staining suggesting unusual mitochondrial function and localization in Pln^{OE} vs WT animals (*51*). This theory may prove relatively easy to assess through a variety of means such as intracellular Ca^{2+} measurement *in vivo* or the manipulation of Ca^{2+} buffering proteins such as parvalbumin (PV). Theoretically, increasing PV content in Pln^{OE} muscles would bind to and buffer excess cytosolic Ca^{2+} and any improvements in the CNM phenotype could then be attributed to improved Ca^{2+} homeostasis with this model.

The second theory that may explain the connection between PLN and a CNM phenotype is the localization of PLN within cellular membranes. Although PLN is classically thought to reside only in the SR membrane, cumulating evidence has found it in other cellular membranes. When assessing PLN in differentiating myocytes, Stenoien et al. (2007), found the localization of PLN varied throughout differentiation with PLN being present in vesicles and then trafficked to

the plasma membrane for degradation in myoblasts that had yet to fully form SR (*124*). A human mutation in PLN has caused its localization to the plasma membrane in cardiomyocytes where it interacts with the N^+-K^+ ATPase pump (*125*). As well, very recent findings from Chiou et al. (2016), show localization of PLN to the nuclear envelope of mature cardiomyocytes and suggest a role for PLN in nuclear Ca^{2+} dynamics (*126*). Although entirely speculative, an overexpression of PLN may promote its localization to other cellular membranes and/or vesicles, which may disrupt normal membrane dynamics within muscle fibres. Interestingly, autophagy, a cell degradation process in which a double membrane vesicle, or autophagosome, engulfs a target organelle or protein aggregate for degradation, was shown to be the primary mode for PLN degradation in cardiomyocytes (*127, 128*). Disrupted autophagy has already been linked to CNM by increased levels of a phosphatase known to initiate autophagy, PtdIns(3)P, and markers for autophagosome membrane development, LC3-I and LC3-II, along with elevation of the lysosomal marker, Lamp2, implicating a late stage halt in the autophagy process within MTM1 mice (*129*). Tempered autophagy in response to starvation was also found in mice with DNM2 mutations, which corresponds with the autosomal dominant form of CNM (*130*), which is the form modeled by Pln^{OE} mice. In relation to the Pln^{OE} CNM model, Fajardo et al, found an increase in LC3II as well as a trending increase in the ratio of LC3II to LC3I, in *C57* black animals harbouring the same pln^{OE} transgene, suggesting alterations in the autophagy process within this model as well (*51*). Together the above data give credence to a mechanism for PLN to cause a CNM phenotype via disruption in regulation of basal autophagy levels.

Furthermore, membrane dysfunction is indicated through notable abnormalities in dystrophin staining upon immunofluorescence imaging of muscles from differing mouse backgrounds overexpressing PLN. Normally, dystrophin is associated with the sarcolemmal

membrane surrounding muscle fibres, but as can be seen in Fig. 11, dystrophin was found within several muscle fibres either alone or surrounding central nuclei. The process by which this dystrophin is incorrectly localized is not known but is assumed not to be non-specific binding as the pattern of expression is seen across mouse strains and experiments. In conjunction with the above evidence, nearly all of the genetic mutations associated with human cases of CNM are associated with a disruption in membrane trafficking, and as such this theory deserves serious review. Future studies could assess PLN localization through immunofluorescence or western blotting of cellular fractions. Future research focused on more clearly defining this process by which increased PLN causes CNM in this model is clearly necessary as it may lead to a strategy to address the increase in PLN expression in human patients with CNM.

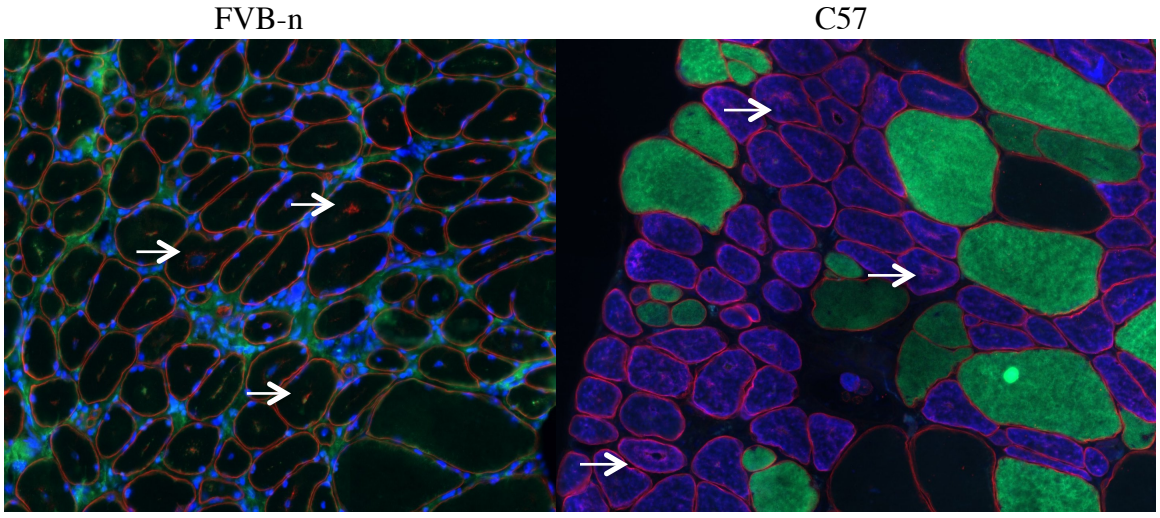

Figure 11. Dystrophin Abnormalities in various Immunofluorescence of Pln^{OE} animals. Immunofluorescence for NFAT, DAPI and Dystrophin from Pln^{OE} animals on an FVB-n strain of mice and Immunofluorescence for MHCI, MHCIIa and Dystrophin from Pln^{OE} animals on a C57 mouse. As denoted by the white arrows both strains and experiments show central localization of dystrophin within muscle fibres.

While the mechanism driving the CNM phenotype in Pln^{OE} mice is currently unknown, the increase in PLN content within biopsies from human patients with CNM shows this relationship is not confined to murine muscle. As such, future studies could also evaluate the

merit of treatments, which more directly target PLN in patients. As Ca^{2+} dysregulation is associated with detrimental myopathic features, and PLN exacerbates this by inhibiting SERCA function and delaying SR Ca^{2+} uptake, targeting PLN directly may prove more fruitful than targeting downstream pathways as in this thesis. A potential treatment, which would directly inhibit PLN and improve SERCA function is via B-agonist administration through activation of PKA and consequent phosphorylation of PLN. Phosphorylation of PLN, shown to weaken its inhibition of SERCA2a (*44*), has been used as a strategy in cardiac muscle, increasing the apparent Ca^{2+} affinity and enhancing relaxation during β-adrenergic stimulation (*45, 46*).

Further research into the CnA- NFAT pathway and its role within CNM is also required. To our knowledge, this is the first study to provide evidence that CnA is over-activated and NFAT may be localized within the nucleus within any model for CNM. We have previously shown that the activation of CnA and localization of NFAT varies between tissues in Pln^{OE} mice compared to WT, as nuclear NFAT was significantly increased in gluteus minimus, a trending increase was found in soleus and no difference was seen in diaphragm muscles (*84*). As such, treatment with CsA may be more effective in one tissue over another. Although this thesis focused on the soleus muscle, preliminary data seen in Fig. 12, suggest that this treatment may have had more of an effect on other postural muscles as noted by the drastic reduction in PLN within CsA-treated gluteus minimus muscles. Exploring the role of the CnA-NFAT pathway within different muscle groups and between models may provide additional insight into its effectiveness as a target for therapeutic strategy.

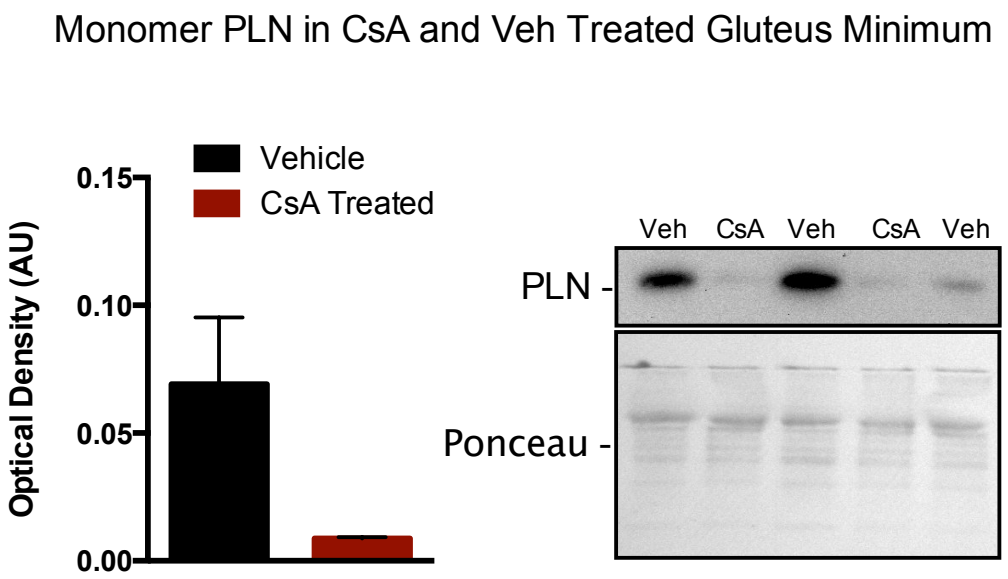

Figure 12. CsA treatment on PLN expression in Gluteus Minimus of *Pln*^{OE} animals. Quantification and full membrane image of the comparison of monomer PLN in gluteus minimus muscle of 4-6 month of *Pln*^{OE} animals treated with CsA or vehicle. Monomer PLN was normalized to total protein via ponceau stain. Statistical significance was not found due to the low power (n = 3 vs 2) and the variance in vehicle treated samples.

As the exact mechanisms driving the differing CNM classifications are still being uncovered, there has yet to be any form of treatment for CNM patients outside of physiotherapy. This study provides evidence that CsA treatment induces modest yet significant benefits as a treatment for CNM in *Pln*^{OE} mice, including increased muscle function, decreased intracellular fibrosis and a mild restoration of fibre type distribution. Targeting fibre type as a potential treatment is both a novel concept and has merit as a universal treatment for CNM patients as the predominance of diseased type I fibres is a phenotype characteristic common to all classifications of CNM. Although this study does not provide enough evidence to suggest that CsA treatment should be examined in human CNM patients, it does provide merit and proof of concept for the targeting of fibre type as a potential avenue for therapeutic strategy.

References

1. N. A. Beard, D. R. Laver, A. F. Dulhunty, Calsequestrin and the calcium release channel of skeletal and cardiac muscle. *Progress in biophysics and molecular biology* **85**, 33-69 (2004); published online EpubMay (10.1016/j.pbiomolbio.2003.07.001).
2. S. Schiaffino, C. Reggiani, Fiber types in mammalian skeletal muscles. *Physiological reviews* **91**, 1447-1531 (2011); published online EpubOct (10.1152/physrev.00031.2010).
3. J. M. East, Sarco(endo)plasmic reticulum calcium pumps: recent advances in our understanding of structure/function and biology (review). *Molecular membrane biology* **17**, 189-200 (2000); published online EpubOct-Dec (
4. M. A. Shareef, L. A. Anwer, C. Poizat, Cardiac SERCA2A/B: therapeutic targets for heart failure. *European journal of pharmacology* **724**, 1-8 (2014); published online EpubFeb 5 (10.1016/j.ejphar.2013.12.018).
5. P. Gailly, New aspects of calcium signaling in skeletal muscle cells: implications in Duchenne muscular dystrophy. *Biochimica et biophysica acta* **1600**, 38-44 (2002); published online EpubNov 4 (S1570963902004429 [pii]).
6. C. J. Brandl, S. deLeon, D. R. Martin, D. H. MacLennan, Adult forms of the Ca2+ATPase of sarcoplasmic reticulum. Expression in developing skeletal muscle. *The Journal of biological chemistry* **262**, 3768-3774 (1987); published online EpubMar 15 (
7. C. J. Brandl, N. M. Green, B. Korczak, D. H. MacLennan, Two Ca2+ ATPase genes: homologies and mechanistic implications of deduced amino acid sequences. *Cell* **44**, 597-607 (1986); published online EpubFeb 28 (
8. J. Lytton, M. Westlin, S. E. Burk, G. E. Shull, D. H. MacLennan, Functional comparisons between isoforms of the sarcoplasmic or endoplasmic reticulum family of calcium pumps. *The Journal of biological chemistry* **267**, 14483-14489 (1992); published online EpubJul 15 (
9. J. Lytton, A. Zarain-Herzberg, M. Periasamy, D. H. MacLennan, Molecular cloning of the mammalian smooth muscle sarco(endo)plasmic reticulum Ca2+-ATPase. *The Journal of biological chemistry* **264**, 7059-7065 (1989); published online EpubApr 25 (
10. P. Szentesi, R. Zaremba, W. van Mechelen, G. J. M. Stienen, ATP utilization for calcium uptake and force production in different types of human skeletal muscle fibres. *J Physiol-London* **531**, 393-403 (2001); published online EpubMar 1 (Doi 10.1111/J.1469-7793.2001.0393i.X).
11. C. Toyoshima, G. Inesi, Structural basis of ion pumping by Ca2+-ATPase of the sarcoplasmic reticulum. *Annual review of biochemistry* **73**, 269-292 (2004)10.1146/annurev.biochem.73.011303.073700).
12. A. G. Lee, Ca2+ -ATPase structure in the E1 and E2 conformations: mechanism, helix-helix and helix-lipid interactions. *Biochimica et biophysica acta* **1565**, 246-266 (2002); published online EpubOct 11 (
13. M. Asahi, Y. Sugita, K. Kurzydlowski, S. De Leon, M. Tada, C. Toyoshima, D. H. MacLennan, Sarcolipin regulates sarco(endo)plasmic reticulum Ca2+-ATPase (SERCA) by binding to transmembrane helices alone or in association with phospholamban. *Proceedings of the National Academy of Sciences of the United States*

of America **100**, 5040-5045 (2003); published online EpubApr 29 (10.1073/pnas.0330962100
0330962100 [pii]).
14. A. Wawrzynow, J. L. Theibert, C. Murphy, I. Jona, A. Martonosi, J. H. Collins, Sarcolipin, the "proteolipid" of skeletal muscle sarcoplasmic reticulum, is a unique, amphipathic, 31-residue peptide. *Archives of biochemistry and biophysics* **298**, 620-623 (1992); published online EpubNov 1 (
15. T. Toyofuku, K. Kurzydlowski, M. Tada, D. H. MacLennan, Identification of regions in the Ca(2+)-ATPase of sarcoplasmic reticulum that affect functional association with phospholamban. *The Journal of biological chemistry* **268**, 2809-2815 (1993); published online EpubFeb 5 (
16. A. Odermatt, S. Becker, V. K. Khanna, K. Kurzydlowski, E. Leisner, D. Pette, D. H. MacLennan, Sarcolipin regulates the activity of SERCA1, the fast-twitch skeletal muscle sarcoplasmic reticulum Ca2+-ATPase. *The Journal of biological chemistry* **273**, 12360-12369 (1998); published online EpubMay 15 (
17. W. S. Smith, R. Broadbridge, J. M. East, A. G. Lee, Sarcolipin uncouples hydrolysis of ATP from accumulation of Ca2+ by the Ca2+-ATPase of skeletal-muscle sarcoplasmic reticulum. *The Biochemical journal* **361**, 277-286 (2002); published online EpubJan 15 (
18. S. K. Sahoo, S. A. Shaikh, D. H. Sopariwala, N. C. Bal, M. Periasamy, Sarcolipin protein interaction with sarco(endo)plasmic reticulum Ca2+ ATPase (SERCA) is distinct from phospholamban protein, and only sarcolipin can promote uncoupling of the SERCA pump. *The Journal of biological chemistry* **288**, 6881-6889 (2013); published online EpubMar 8 (10.1074/jbc.M112.436915
M112.436915 [pii]).
19. J. Fujii, K. Maruyama, M. Tada, D. H. MacLennan, Co-expression of slow-twitch/cardiac muscle Ca2(+)-ATPase (SERCA2) and phospholamban. *FEBS letters* **273**, 232-234 (1990); published online EpubOct 29 (
20. V. A. Fajardo, E. Bombardier, C. Vigna, T. Devji, D. Bloemberg, D. Gamu, A. O. Gramolini, J. Quadrilatero, A. R. Tupling, Co-Expression of SERCA Isoforms, Phospholamban and Sarcolipin in Human Skeletal Muscle Fibers. *PloS one* **8**, e84304 (2013)10.1371/journal.pone.0084304
PONE-D-13-25403 [pii]).
21. M. Asahi, K. Kurzydlowski, M. Tada, D. H. MacLennan, Sarcolipin inhibits polymerization of phospholamban to induce superinhibition of sarco(endo)plasmic reticulum Ca2+-ATPases (SERCAs). *The Journal of biological chemistry* **277**, 26725-26728 (2002); published online EpubJul 26 (10.1074/jbc.C200269200
C200269200 [pii]).
22. D. M. Anderson, K. M. Anderson, C. L. Chang, C. A. Makarewich, B. R. Nelson, J. R. McAnally, P. Kasaragod, J. M. Shelton, J. Liou, R. Bassel-Duby, E. N. Olson, A Micropeptide Encoded by a Putative Long Noncoding RNA Regulates Muscle Performance. *Cell*, (2015); published online EpubJan 28 (10.1016/j.cell.2015.01.009).
23. B. R. Nelson, C. A. Makarewich, D. M. Anderson, B. R. Winders, C. D. Troupes, F. Wu, A. L. Reese, J. R. McAnally, X. Chen, E. T. Kavalali, S. C. Cannon, S. R. Houser, R. Bassel-Duby, E. N. Olson, A peptide encoded by a transcript annotated as long noncoding

RNA enhances SERCA activity in muscle. *Science* **351**, 271-275 (2016); published online EpubJan 15 (10.1126/science.aad4076).
24. V. Sivakumaran, B. A. Stanley, C. G. Tocchetti, J. D. Ballin, V. Caceres, L. Zhou, G. Keceli, P. P. Rainer, D. I. Lee, S. Huke, M. T. Ziolo, E. G. Kranias, J. P. Toscano, G. M. Wilson, B. O'Rourke, D. A. Kass, J. E. Mahaney, N. Paolocci, HNO enhances SERCA2a activity and cardiomyocyte function by promoting redox-dependent phospholamban oligomerization. *Antioxidants & redox signaling* **19**, 1185-1197 (2013); published online EpubOct 10 (10.1089/ars.2012.5057).
25. R. I. Viner, T. D. Williams, C. Schoneich, Peroxynitrite modification of protein thiols: oxidation, nitrosylation, and S-glutathiolation of functionally important cysteine residue(s) in the sarcoplasmic reticulum Ca-ATPase. *Biochemistry* **38**, 12408-12415 (1999); published online EpubSep 21 (bi9909445 [pii]).
26. E. Babusikova, J. Lehotsky, D. Dobrota, P. Racay, P. Kaplan, Age-associated changes in Ca(2+)-ATPase and oxidative damage in sarcoplasmic reticulum of rat heart. *Physiological research / Academia Scientiarum Bohemoslovaca* **61**, 453-460 (2012).
27. A. R. Tupling, A. O. Gramolini, T. A. Duhamel, H. Kondo, M. Asahi, S. C. Tsuchiya, M. J. Borrelli, J. R. Lepock, K. Otsu, M. Hori, D. H. MacLennan, H. J. Green, HSP70 binds to the fast-twitch skeletal muscle sarco(endo)plasmic reticulum Ca2+ -ATPase (SERCA1a) and prevents thermal inactivation. *The Journal of biological chemistry* **279**, 52382-52389 (2004); published online EpubDec 10 (10.1074/jbc.M409336200
M409336200 [pii]).
28. B. De Paepe, K. K. Creus, J. Weis, J. L. De Bleecker, Heat shock protein families 70 and 90 in Duchenne muscular dystrophy and inflammatory myopathy: Balancing muscle protection and destruction. *Neuromuscular Disord* **22**, 26-33 (2012); published online EpubJan (10.1016/j.nmd.2011.07.007).
29. E. G. Kranias, D. M. Bers, Calcium and cardiomyopathies. *Sub-cellular biochemistry* **45**, 523-537 (2007).
30. J. S. Schneider, M. Shanmugam, J. P. Gonzalez, H. Lopez, R. Gordan, D. Fraidenraich, G. J. Babu, Increased sarcolipin expression and decreased sarco(endo)plasmic reticulum Ca2+ uptake in skeletal muscles of mouse models of Duchenne muscular dystrophy. *Journal of muscle research and cell motility* **34**, 349-356 (2013); published online EpubDec (10.1007/s10974-013-9350-0).
31. S. A. Goonasekera, C. K. Lam, D. P. Millay, M. A. Sargent, R. J. Hajjar, E. G. Kranias, J. D. Molkentin, Mitigation of muscular dystrophy in mice by SERCA overexpression in skeletal muscle. *The Journal of clinical investigation* **121**, 1044-1052 (2011); published online EpubMar (10.1172/JCI43844
43844 [pii]).
32. S. M. Gehrig, C. van der Poel, T. A. Sayer, J. D. Schertzer, D. C. Henstridge, J. E. Church, S. Lamon, A. P. Russell, K. E. Davies, M. A. Febbraio, G. S. Lynch, Hsp72 preserves muscle function and slows progression of severe muscular dystrophy. *Nature* **484**, 394-398 (2012); published online EpubApr 19 (10.1038/nature10980
nature10980 [pii]).
33. P. Bhupathy, G. J. Babu, M. Periasamy, Sarcolipin and phospholamban as regulators of cardiac sarcoplasmic reticulum Ca2+ ATPase. *Journal of molecular and cellular*

cardiology **42**, 903-911 (2007); published online EpubMay (S0022-2828(07)00791-2 [pii]
10.1016/j.yjmcc.2007.03.738).
34. K. Haghighi, F. Kolokathis, A. O. Gramolini, J. R. Waggoner, L. Pater, R. A. Lynch, G. C. Fan, D. Tsiapras, R. R. Parekh, G. W. Dorn, 2nd, D. H. MacLennan, D. T. Kremastinos, E. G. Kranias, A mutation in the human phospholamban gene, deleting arginine 14, results in lethal, hereditary cardiomyopathy. *Proceedings of the National Academy of Sciences of the United States of America* **103**, 1388-1393 (2006); published online EpubJan 31 (0510519103 [pii]
10.1073/pnas.0510519103).
35. J. P. Schmitt, M. Kamisago, M. Asahi, G. H. Li, F. Ahmad, U. Mende, E. G. Kranias, D. H. MacLennan, J. G. Seidman, C. E. Seidman, Dilated cardiomyopathy and heart failure caused by a mutation in phospholamban. *Science* **299**, 1410-1413 (2003); published online EpubFeb 28 (10.1126/science.1081578
299/5611/1410 [pii]).
36. N. J. Traaseth, L. Shi, R. Verardi, D. G. Mullen, G. Barany, G. Veglia, Structure and topology of monomeric phospholamban in lipid membranes determined by a hybrid solution and solid-state NMR approach. *Proceedings of the National Academy of Sciences of the United States of America* **106**, 10165-10170 (2009); published online EpubJun 23 (10.1073/pnas.0904290106).
37. S. Smeazzetto, F. Tadini-Buoninsegni, G. Thiel, D. Berti, C. Montis, Phospholamban spontaneously reconstitutes into giant unilamellar vesicles where it generates a cation selective channel. *Physical chemistry chemical physics : PCCP* **18**, 1629-1636 (2016); published online EpubJan 21 (10.1039/c5cp05893g).
38. T. Wittmann, M. J. Lohse, J. P. Schmitt, Phospholamban pentamers attenuate PKA-dependent phosphorylation of monomers. *Journal of molecular and cellular cardiology* **80**, 90-97 (2015); published online EpubMar (10.1016/j.yjmcc.2014.12.020).
39. H. K. Simmerman, J. H. Collins, J. L. Theibert, A. D. Wegener, L. R. Jones, Sequence analysis of phospholamban. Identification of phosphorylation sites and two major structural domains. *The Journal of biological chemistry* **261**, 13333-13341 (1986); published online EpubOct 5 (
40. K. L. Koss, E. G. Kranias, Phospholamban: a prominent regulator of myocardial contractility. *Circulation research* **79**, 1059-1063 (1996); published online EpubDec (
41. W. Luo, I. L. Grupp, J. Harrer, S. Ponniah, G. Grupp, J. J. Duffy, T. Doetschman, E. G. Kranias, Targeted ablation of the phospholamban gene is associated with markedly enhanced myocardial contractility and loss of beta-agonist stimulation. *Circulation research* **75**, 401-409 (1994); published online EpubSep (
42. B. M. Wolska, M. O. Stojanovic, W. Luo, E. G. Kranias, R. J. Solaro, Effect of ablation of phospholamban on dynamics of cardiac myocyte contraction and intracellular Ca2+. *The American journal of physiology* **271**, C391-397 (1996); published online EpubJul (
43. J. P. Slack, I. L. Grupp, W. Luo, E. G. Kranias, Phospholamban ablation enhances relaxation in the murine soleus. *The American journal of physiology* **273**, C1-6 (1997); published online EpubJul (

44. Z. Chen, B. L. Akin, L. R. Jones, Mechanism of reversal of phospholamban inhibition of the cardiac Ca2+-ATPase by protein kinase A and by anti-phospholamban monoclonal antibody 2D12. *The Journal of biological chemistry* **282**, 20968-20976 (2007); published online EpubJul 20 (10.1074/jbc.M703516200).
45. L. Li, J. Desantiago, G. Chu, E. G. Kranias, D. M. Bers, Phosphorylation of phospholamban and troponin I in beta-adrenergic-induced acceleration of cardiac relaxation. *American journal of physiology. Heart and circulatory physiology* **278**, H769-779 (2000); published online EpubMar (
46. G. Chu, J. W. Lester, K. B. Young, W. Luo, J. Zhai, E. G. Kranias, A single site (Ser16) phosphorylation in phospholamban is sufficient in mediating its maximal cardiac responses to beta -agonists. *The Journal of biological chemistry* **275**, 38938-38943 (2000); published online EpubDec 8 (10.1074/jbc.M004079200
M004079200 [pii]).
47. K. Haghighi, A. G. Schmidt, B. D. Hoit, A. G. Brittsan, A. Yatani, J. W. Lester, J. Zhai, Y. Kimura, G. W. Dorn, 2nd, D. H. MacLennan, E. G. Kranias, Superinhibition of sarcoplasmic reticulum function by phospholamban induces cardiac contractile failure. *The Journal of biological chemistry* **276**, 24145-24152 (2001); published online EpubJun 29 (10.1074/jbc.M102403200
M102403200 [pii]).
48. S. Minamisawa, Y. Sato, Y. Tatsuguchi, T. Fujino, S. Imamura, Y. Uetsuka, M. Nakazawa, R. Matsuoka, Mutation of the phospholamban promoter associated with hypertrophic cardiomyopathy. *Biochemical and biophysical research communications* **304**, 1-4 (2003); published online EpubApr 25 (S0006291X03005266 [pii]).
49. J. S. Pattison, J. R. Waggoner, J. James, L. Martin, J. Gulick, H. Osinska, R. Klevitsky, E. G. Kranias, J. Robbins, Phospholamban overexpression in transgenic rabbits. *Transgenic research* **17**, 157-170 (2008); published online EpubApr (10.1007/s11248-007-9139-2).
50. Q. Song, K. B. Young, G. Chu, J. Gulick, M. Gerst, I. L. Grupp, J. Robbins, E. G. Kranias, Overexpression of phospholamban in slow-twitch skeletal muscle is associated with depressed contractile function and muscle remodeling. *FASEB journal : official publication of the Federation of American Societies for Experimental Biology* **18**, 974-976 (2004); published online EpubJun (10.1096/fj.03-1058fje
03-1058fje [pii]).
51. V. A. Fajardo, E. Bombardier, E. McMillan, K. Tran, B. J. Wadsworth, D. Gamu, A. Hopf, C. Vigna, I. C. Smith, C. Bellissimo, R. N. Michel, M. A. Tarnopolsky, J. Quadrilatero, A. R. Tupling, Phospholamban overexpression in mice causes a centronuclear myopathy-like phenotype. *Disease models & mechanisms* **8**, 999-1009 (2015); published online EpubAug 1 (10.1242/dmm.020859).
52. A. J. Spiro, G. M. Shy, N. K. Gonatas, Myotubular myopathy. Persistence of fetal muscle in an adolescent boy. *Archives of neurology* **14**, 1-14 (1966); published online EpubJan (
53. A. H. Beggs, J. Bohm, E. Snead, M. Kozlowski, M. Maurer, K. Minor, M. K. Childers, S. M. Taylor, C. Hitte, J. R. Mickelson, L. T. Guo, A. P. Mizisin, A. Buj-Bello, L. Tiret, J. Laporte, G. D. Shelton, MTM1 mutation associated with X-linked myotubular myopathy in Labrador Retrievers. *Proceedings of the National Academy of Sciences of*

the United States of America **107**, 14697-14702 (2010); published online EpubAug 17 (10.1073/pnas.1003677107).
54. J. Gurgel-Giannetti, E. Zanoteli, E. L. de Castro Concentino, O. Abath Neto, J. B. Pesquero, U. C. Reed, M. Vainzof, Necklace fibers as histopathological marker in a patient with severe form of X-linked myotubular myopathy. *Neuromuscular disorders : NMD* **22**, 541-545 (2012); published online EpubJun (10.1016/j.nmd.2011.12.005).
55. L. Amoasii, D. L. Bertazzi, H. Tronchere, K. Hnia, G. Chicanne, B. Rinaldi, B. S. Cowling, A. Ferry, B. Klaholz, B. Payrastre, J. Laporte, S. Friant, Phosphatase-dead myotubularin ameliorates X-linked centronuclear myopathy phenotypes in mice. *PLoS genetics* **8**, e1002965 (2012)10.1371/journal.pgen.1002965).
56. H. Jungbluth, M. Gautel, Pathogenic mechanisms in centronuclear myopathies. *Frontiers in aging neuroscience* **6**, 339 (2014)10.3389/fnagi.2014.00339).
57. L. J. Hu, J. Laporte, W. Kress, P. Kioschis, R. Siebenhaar, A. Poustka, M. Fardeau, A. Metzenberg, E. A. Janssen, N. Thomas, J. L. Mandel, N. Dahl, Deletions in Xq28 in two boys with myotubular myopathy and abnormal genital development define a new contiguous gene syndrome in a 430 kb region. *Human molecular genetics* **5**, 139-143 (1996); published online EpubJan (Doi 10.1093/Hmg/5.1.139).
58. R. Joubert, A. Vignaud, M. Le, C. Moal, N. Messaddeq, A. Buj-Bello, Site-specific Mtm1 mutagenesis by an AAV-Cre vector reveals that myotubularin is essential in adult muscle. *Human molecular genetics* **22**, 1856-1866 (2013); published online EpubMay 1 (10.1093/hmg/ddt038).
59. J. Laporte, V. Biancalana, S. M. Tanner, W. Kress, V. Schneider, C. Wallgren-Pettersson, F. Herger, A. Buj-Bello, F. Blondeau, S. Liechti-Gallati, J. L. Mandel, MTM1 mutations in X-linked myotubular myopathy. *Human mutation* **15**, 393-409 (2000)10.1002/(SICI)1098-1004(200005)15:5<393::AID-HUMU1>3.0.CO;2-R).
60. L. Wang, B. Barylko, C. Byers, J. A. Ross, D. M. Jameson, J. P. Albanesi, Dynamin 2 mutants linked to centronuclear myopathies form abnormally stable polymers. *The Journal of biological chemistry* **285**, 22753-22757 (2010); published online EpubJul 23 (10.1074/jbc.C110.130013).
61. D. Fischer, M. Herasse, M. Bitoun, H. M. Barragan-Campos, J. Chiras, P. Laforet, M. Fardeau, B. Eymard, P. Guicheney, N. B. Romero, Characterization of the muscle involvement in dynamin 2-related centronuclear myopathy. *Brain : a journal of neurology* **129**, 1463-1469 (2006); published online EpubJun (10.1093/brain/awl071).
62. M. Bitoun, S. Maugenre, P. Y. Jeannet, E. Lacene, X. Ferrer, P. Laforet, J. J. Martin, J. Laporte, H. Lochmuller, A. H. Beggs, M. Fardeau, B. Eymard, N. B. Romero, P. Guicheney, Mutations in dynamin 2 cause dominant centronuclear myopathy. *Nature genetics* **37**, 1207-1209 (2005); published online EpubNov (ng1657 [pii] 10.1038/ng1657).
63. M. Mori-Yoshimura, A. Okuma, Y. Oya, C. Fujimura-Kiyono, H. Nakajima, K. Matsuura, A. Takemura, M. C. Malicdan, Y. K. Hayashi, I. Nonaka, M. Murata, I. Nishino, Clinicopathological features of centronuclear myopathy in Japanese populations harboring mutations in dynamin 2. *Clinical neurology and neurosurgery* **114**, 678-683 (2012); published online EpubJul (10.1016/j.clineuro.2011.10.040).

64. C. Fugier, A. F. Klein, C. Hammer, S. Vassilopoulos, Y. Ivarsson, A. Toussaint, V. Tosch, A. Vignaud, A. Ferry, N. Messaddeq, Y. Kokunai, R. Tsuburaya, P. de la Grange, D. Dembele, V. Francois, G. Precigout, C. Boulade-Ladame, M. C. Hummel, A. Lopez de Munain, N. Sergeant, A. Laquerriere, C. Thibault, F. Deryckere, D. Auboeuf, L. Garcia, P. Zimmermann, B. Udd, B. Schoser, M. P. Takahashi, I. Nishino, G. Bassez, J. Laporte, D. Furling, N. Charlet-Berguerand, Misregulated alternative splicing of BIN1 is associated with T tubule alterations and muscle weakness in myotonic dystrophy. *Nature medicine* **17**, 720-725 (2011); published online EpubJun (10.1038/nm.2374).
65. H. Jungbluth, H. Zhou, C. A. Sewry, S. Robb, S. Treves, M. Bitoun, P. Guicheney, A. Buj-Bello, C. Bonnemann, F. Muntoni, Centronuclear myopathy due to a de novo dominant mutation in the skeletal muscle ryanodine receptor (RYR1) gene. *Neuromuscular disorders : NMD* **17**, 338-345 (2007); published online EpubApr (S0960-8966(07)00021-1 [pii]
10.1016/j.nmd.2007.01.016).
66. H. Jungbluth, C. Wallgren-Pettersson, J. Laporte, Centronuclear (myotubular) myopathy. *Orphanet J Rare Dis* **3**, 26 (2008)10.1186/1750-1172-3-26
1750-1172-3-26 [pii]).
67. M. S. Deangelis, L. Palmucci, M. Leone, C. Doriguzzi, Centronuclear Myopathy - Clinical, Morphological and Genetic Characters - a Review of 288 Cases. *J Neurol Sci* **103**, 2-9 (1991); published online EpubMay (Doi 10.1016/0022-510x(91)90275-C).
68. N. Liu, S. Bezprozvannaya, J. M. Shelton, M. I. Frisard, M. W. Hulver, R. P. McMillan, Y. Wu, K. A. Voelker, R. W. Grange, J. A. Richardson, R. Bassel-Duby, E. N. Olson, Mice lacking microRNA 133a develop dynamin 2-dependent centronuclear myopathy. *The Journal of clinical investigation* **121**, 3258-3268 (2011); published online EpubAug (10.1172/JCI46267
46267 [pii]).
69. M. W. Lawlor, B. P. Read, R. Edelstein, N. Yang, C. R. Pierson, M. J. Stein, A. Wermer-Colan, A. Buj-Bello, J. L. Lachey, J. S. Seehra, A. H. Beggs, Inhibition of activin receptor type IIB increases strength and lifespan in myotubularin-deficient mice. *The American journal of pathology* **178**, 784-793 (2011); published online EpubFeb (10.1016/j.ajpath.2010.10.035).
70. L. L. Smith, V. A. Gupta, A. H. Beggs, Bridging integrator 1 (Bin1) deficiency in zebrafish results in centronuclear myopathy. *Human molecular genetics* **23**, 3566-3578 (2014); published online EpubJul 1 (10.1093/hmg/ddu067).
71. A. C. Durieux, A. Vignaud, B. Prudhon, M. T. Viou, M. Beuvin, S. Vassilopoulos, B. Fraysse, A. Ferry, J. Laine, N. B. Romero, P. Guicheney, M. Bitoun, A centronuclear myopathy-dynamin 2 mutation impairs skeletal muscle structure and function in mice. *Human molecular genetics* **19**, 4820-4836 (2010); published online EpubDec 15 (10.1093/hmg/ddq413
ddq413 [pii]).
72. C. B. Klee, T. H. Crouch, M. H. Krinks, Calcineurin: a calcium- and calmodulin-binding protein of the nervous system. *Proceedings of the National Academy of Sciences of the United States of America* **76**, 6270-6273 (1979); published online EpubDec (

73. **R. F. Rumi-Masante J, Lester TE, Dunlap TB, Williams TD, Dunker AK, Weis DD, Creamer TP**, Structural basis for activation of calcineurin by calmodulin. *Journal of molecular biology* **415**, 307-317 (2012).
74. L. C. Rao A., Hogan PG., Transcription factors of the NFAT family: regulation and function. *Annual Review of Immunology* **15**, 707-747 (1997).
75. P. G. Hogan, L. Chen, J. Nardone, A. Rao, Transcriptional regulation by calcium, calcineurin, and NFAT. *Genes & development* **17**, 2205-2232 (2003); published online EpubSep 15 (10.1101/gad.1102703).
76. N. A. Clipstone, G. R. Crabtree, Identification of calcineurin as a key signalling enzyme in T-lymphocyte activation. *Nature* **357**, 695-697 (1992); published online EpubJun 25 (10.1038/357695a0).
77. B. B. Friday, V. Horsley, G. K. Pavlath, Calcineurin activity is required for the initiation of skeletal muscle differentiation. *The Journal of cell biology* **149**, 657-666 (2000); published online EpubMay 1 (
78. V. Horsley, B. B. Friday, S. Matteson, K. M. Kegley, J. Gephart, G. K. Pavlath, Regulation of the growth of multinucleated muscle cells by an NFATC2-dependent pathway. *The Journal of cell biology* **153**, 329-338 (2001); published online EpubApr 16 (
79. F. J. Naya, Stimulation of Slow Skeletal Muscle Fiber Gene Expression by Calcineurin in Vivo. *Journal of Biological Chemistry* **275**, 4545-4548 (2000)10.1074/jbc.275.7.4545).
80. R. J. Talmadge, J. S. Otis, M. R. Rittler, N. D. Garcia, S. R. Spencer, S. J. Lees, F. J. Naya, Calcineurin activation influences muscle phenotype in a muscle-specific fashion. *BMC Cell Biol* **5**, 28 (2004); published online EpubJul 28 (10.1186/1471-2121-5-28 1471-2121-5-28 [pii]).
81. K. J. McCullagh, E. Calabria, G. Pallafacchina, S. Ciciliot, A. L. Serrano, C. Argentini, J. M. Kalhovde, T. Lomo, S. Schiaffino, NFAT is a nerve activity sensor in skeletal muscle and controls activity-dependent myosin switching. *Proceedings of the National Academy of Sciences of the United States of America* **101**, 10590-10595 (2004); published online EpubJul 20 (10.1073/pnas.0308035101).
82. J. Ochala, L. Larsson, in *Muscle,* J. A. Hill, E. N. Olson, Eds. (Academic Press, Boston/Waltham, 2012), pp. 1023-1030.
83. J. V. Chakkalakal, M. A. Stocksley, M. A. Harrison, L. M. Angus, J. Deschenes-Furry, S. St-Pierre, L. A. Megeney, E. R. Chin, R. N. Michel, B. J. Jasmin, Expression of utrophin A mRNA correlates with the oxidative capacity of skeletal muscle fiber types and is regulated by calcineurin/NFAT signaling. *Proceedings of the National Academy of Sciences of the United States of America* **100**, 7791-7796 (2003); published online EpubJun 24 (10.1073/pnas.0932671100).
84. V. A. Fajardo, Smith, I.C., Bombardier, E., Chambers, P.J., Tupling, A.R. , Diaphragm assessment in mice overexpressing phospholamban in slow-twitch type I muscle fibers. *Brain and behavior* **6**, (2016).
85. C. E. Torgan, M. P. Daniels, Regulation of myosin heavy chain expression during rat skeletal muscle development in vitro. *Molecular biology of the cell* **12**, 1499-1508 (2001); published online EpubMay (
86. S. E. Dunn, E. R. Chin, R. N. Michel, Matching of calcineurin activity to upstream effectors is critical for skeletal muscle fiber growth. *The Journal of cell biology* **151**, 663-672 (2000); published online EpubOct 30 (

87. A. B. Nicolli, E. Petronilli, V. Wenger, R.M. Bernardi, P., Interactions of Cyclophilin with Mitochondrial Inner Membrane and Regulation of the Permeability Transition Pore, a Cyclosporin A-sensitive Channel. *Journal of Biological Chemistry* **271**, 2185-2192 (1996).
88. A. Laupacis, P. A. Keown, R. A. Ulan, N. McKenzie, C. R. Stiller, Cyclosporin A: a powerful immunosuppressant. *Canadian Medical Association journal* **126**, 1041-1046 (1982); published online EpubMay 1 (
89. D. Bloemberg, J. Quadrilatero, Rapid determination of myosin heavy chain expression in rat, mouse, and human skeletal muscle using multicolor immunofluorescence analysis. *PloS one* **7**, e35273 (2012)10.1371/journal.pone.0035273
PONE-D-11-20138 [pii]).
90. T. A. Duhamel, H. J. Green, R. D. Stewart, K. P. Foley, I. C. Smith, J. Ouyang, Muscle metabolic, SR Ca(2+) -cycling responses to prolonged cycling, with and without glucose supplementation. *Journal of applied physiology* **103**, 1986-1998 (2007); published online EpubDec (01440.2006 [pii]
10.1152/japplphysiol.01440.2006).
91. F. Jaskolski, C. Mulle, O. J. Manzoni, An automated method to quantify and visualize colocalized fluorescent signals. *Journal of neuroscience methods* **146**, 42-49 (2005); published online EpubJul 15 (10.1016/j.jneumeth.2005.01.012).
92. R. N. Michel, E. R. Chin, J. V. Chakkalakal, J. K. Eibl, B. J. Jasmin, Ca2+/calmodulin-based signalling in the regulation of the muscle fibre phenotype and its therapeutic potential via modulation of utrophin A and myostatin expression. *Applied physiology, nutrition, and metabolism = Physiologie appliquee, nutrition et metabolisme* **32**, 921-929 (2007); published online EpubOct (10.1139/H07-093).
93. M.-J. W. C. Semsarian, Y.-K. Ju, et al. , Skeletal muscle hypertrophy is mediated by Ca2+-dependent calcineurin signalling pathway. *Nature* **400**, 576-581 (1999).
94. S. E. Dunn, J. L. Burns, R. N. Michel, Calcineurin is required for skeletal muscle hypertrophy. *The Journal of biological chemistry* **274**, 21908-21912 (1999); published online EpubJul 30 (
95. C. Lopez-Rodriguez, J. Aramburu, A. S. Rakeman, A. Rao, NFAT5, a constitutively nuclear NFAT protein that does not cooperate with Fos and Jun. *Proceedings of the National Academy of Sciences of the United States of America* **96**, 7214-7219 (1999); published online EpubJun 22 (Doi 10.1073/Pnas.96.13.7214).
96. A. V. Tsytsykova, A. E. Goldfeld, Nuclear factor of activated T cells transcription factor NFATp controls superantigen-induced lethal shock. *Journal of Experimental Medicine* **192**, 581-586 (2000); published online EpubAug 21 (Doi 10.1084/Jem.192.4.581).
97. J. Luo, L. X. Sun, X. Lin, G. X. Liu, J. Yu, L. Parisiadou, C. S. Xie, J. H. Ding, H. B. Cai, A calcineurin- and NFAT-dependent pathway is involved in alpha-synuclein-induced degeneration of midbrain dopaminergic neurons. *Human molecular genetics* **23**, 6567-6574 (2014); published online EpubDec 15 (10.1093/hmg/ddu377).
98. I. A. Graef, F. Chen, L. Chen, A. Kuo, G. R. Crabtree, Signals transduced by Ca2+/calcineurin and NFATc3/c4 pattern the developing vasculature. *Cell* **105**, 863-875 (2001); published online EpubJun 29 (Doi 10.1016/S0092-8674(01)00396-8).

99. K. Abbott, V. Boss, X. F. Wang, G. K. Pavlath, T. J. Murphy, Differential induction of NFAT-mediated transcription in vascular smooth muscle cells by phospholipase C-coupled cell surface receptors. *Faseb Journal* **12**, A131-A131 (1998); published online EpubMar 17 (
100. K. M. Kegley, J. Gephart, G. L. Warren, G. K. Pavlath, Altered primary myogenesis in NFATC3(-/-) mice leads to decreased muscle size in the adult. *Dev Biol* **232**, 115-126 (2001); published online EpubApr 1 (Doi 10.1006/Dbio.2001.0179).
101. N. Daou, S. Lecolle, S. Lefebvre, B. della Gaspera, F. Charbonnier, C. Chanoine, A. S. Armand, A new role for the calcineurin/NFAT pathway in neonatal myosin heavy chain expression via the NFATc2/MyoD complex during mouse myogenesis. *Development* **140**, 4914-4925 (2013); published online EpubDec (10.1242/dev.097428).
102. M. L. Ehlers, B. Celona, B. L. Black, NFATc1 Controls Skeletal Muscle Fiber Type and Is a Negative Regulator of MyoD Activity. *Cell Rep* **8**, 1639-1648 (2014); published online EpubSep 25 (10.1016/j.celrep.2014.08.035).
103. E. Calabria, S. Ciciliot, I. Moretti, M. Garcia, A. Picard, K. A. Dyar, G. Pallafacchina, J. Tothova, S. Schiaffino, M. Murgia, NFAT isoforms control activity-dependent muscle fiber type specification. *Proceedings of the National Academy of Sciences of the United States of America* **106**, 13335-13340 (2009); published online EpubAug 11 (10.1073/pnas.0812911106).
104. G. R. Crabtree, Generic signals and specific outcomes: Signaling through Ca2+, calcineurin, and NF-AT. *Cell* **96**, 611-614 (1999); published online EpubMar 5 (Doi 10.1016/S0092-8674(00)80571-1).
105. B. Fiedler, K. C. Wollert, Interference of antihypertrophic molecules and signaling pathways with the Ca2+-calcineurin-NFAT cascade in cardiac myocytes. *Cardiovascular research* **63**, 450-457 (2004); published online EpubAug 15 (10.1016/j.cardiores.2004.04.002).
106. A. Okamura, K. Yamamoto, K. Yakushijin, N. Urahama, K. Minagawa, A. Sada, A. Hato, S. Nishikawa, K. Yokoyama, M. Ito, T. Matsui, Casein kinase I epsilon downregulates PI3K/Akt signaling, followed by genotoxic stress-induced apoptosis of hematopoietic cells. *Blood* **104**, 360A-360A (2004); published online EpubNov 16 (
107. V. Boss, K. L. Abbott, X. F. Wang, G. K. Pavlath, T. J. Murphy, The cyclosporin A-sensitive nuclear factor of activated T cells (NFAT) proteins are expressed in vascular smooth muscle cells - Differential localization of NFAT isoforms and induction of NFAT-mediated transcription by phospholipase c-coupled cell surface receptors. *Journal of Biological Chemistry* **273**, 19664-19671 (1998); published online EpubJul 31 (Doi 10.1074/Jbc.273.31.19664).
108. C. W. Chow, C. Dong, R. A. Flavell, R. J. Davis, c-Jun NH(2)-terminal kinase inhibits targeting of the protein phosphatase calcineurin to NFATc1. *Molecular and cellular biology* **20**, 5227-5234 (2000); published online EpubJul (
109. L. A. Timmerman, N. A. Clipstone, S. N. Ho, J. P. Northrop, G. R. Crabtree, Rapid shuttling of NF-AT in discrimination of Ca2+ signals and immunosuppression. *Nature* **383**, 837-840 (1996); published online EpubOct 31 (10.1038/383837a0).
110. K. Stankunas, I. A. Graef, J. R. Neilson, S. H. Park, G. R. Crabtree, Signaling through calcium, calcineurin, and NF-AT in lymphocyte activation and development. *Cold Spring Harb Sym* **64**, 505-516 (1999)Doi 10.1101/Sqb.1999.64.505).

111. A. Odermatt, K. Kurzydlowski, D. H. MacLennan, The vmax of the Ca2+-ATPase of cardiac sarcoplasmic reticulum (SERCA2a) is not altered by Ca2+/calmodulin-dependent phosphorylation or by interaction with phospholamban. *The Journal of biological chemistry* **271**, 14206-14213 (1996); published online EpubJun 14 (
112. L. M. Pan, T. Wang, F. X. Shi, Molecular basis of activation and replenishment on satellite cell shed light on myopathy. *Prog Biochem Biophys* **33**, 811-815 (2006); published online EpubSep (
113. B. S. Cowling, A. Toussaint, L. Amoasii, P. Koebel, A. Ferry, L. Davignon, I. Nishino, J. L. Mandel, J. Laporte, Increased expression of wild-type or a centronuclear myopathy mutant of dynamin 2 in skeletal muscle of adult mice leads to structural defects and muscle weakness. *The American journal of pathology* **178**, 2224-2235 (2011); published online EpubMay (10.1016/j.ajpath.2011.01.054).
114. T. Chen, C. Q. Pu, Q. Wang, J. X. Liu, Y. L. Mao, Q. Shi, Clinical, pathological, and genetic features of dynamin-2-related centronuclear myopathy in China. *Neurol Sci* **36**, 735-741 (2015); published online EpubMay (10.1007/s10072-014-2028-6).
115. V. A. Fajardo, The Role of Phospholamban and Sarcolipin in Skeletal Muscle Disease. *PhD Thesis Dissertation, University of Waterloo* (2015).
116. R. E. Dolmetsch, R. S. Lewis, C. C. Goodnow, J. I. Healy, Differential activation of transcription factors induced by Ca2+ response amplitude and duration. *Nature* **386**, 855-858 (1997); published online EpubApr 24 (10.1038/386855a0).
117. C. Collet, B. Allard, Y. Tourneur, V. Jacquemond, Intracellular calcium signals measured with indo-1 in isolated skeletal muscle fibres from control and mdx mice. *The Journal of physiology* **520 Pt 2**, 417-429 (1999); published online EpubOct 15 (
118. H. J. Helin, T. S. Edgington, Cyclosporin-a Regulates Monocyte Macrophage Effector Functions by Affecting Instructor T-Cells - Inhibition of Monocyte Procoagulant Response to Allogeneic Stimulation. *Journal of immunology* **132**, 1074-1076 (1984).
119. M. Holm, Nielsen, H.K., Andersen, H.B., Schietz, P.O., Junker, S., Chemokine gene expression in CD133 cord blood derived human mast cells and modulation by cyclosporin A and dexamethasone. *Journal of Allergy and Clinical Immunology* **113**, S83 (2004).
120. K. Ina, K. Kusugami, T. Ando, T. Hosokawa, A. Imada, M. Ohsuga, M. Shimada, Cyclosporin A has suppressive effects on neutrophils and mucosal T-cells. *Gastroenterology* **114**, A1002-A1002 (1998); published online EpubApr 15 (Doi 10.1016/S0016-5085(98)84077-8).
121. Q. Meng, S. Ying, C. J. Corrigan, M. Wakelin, B. Assoufi, R. Moqbel, A. B. Kay, Effects of rapamycin, cyclosporin A, and dexamethasone on interleukin 5-induced eosinophil degranulation and prolonged survival. *Allergy* **52**, 1095-1101 (1997); published online EpubNov (Doi 10.1111/J.1398-9995.1997.Tb00181.X).
122. P. R. Turner, T. Westwood, C. M. Regen, R. A. Steinhardt, Increased protein degradation results from elevated free calcium levels found in muscle from mdx mice. *Nature* **335**, 735-738 (1988); published online EpubOct 20 (10.1038/335735a0).
123. A. K. Sharma, B. Rohrer, Calcium-induced calpain mediates apoptosis via caspase-3 in a mouse photoreceptor cell line. *The Journal of biological chemistry* **279**, 35564-35572 (2004); published online EpubAug 20 (10.1074/jbc.M401037200).

124. D. L. Stenoien, T. V. Knyushko, M. P. Londono, L. K. Opresko, M. U. Mayer, S. T. Brady, T. C. Squier, D. J. Bigelow, Cellular trafficking of phospholamban and formation of functional sarcoplasmic reticulum during myocyte differentiation. *American journal of physiology. Cell physiology* **292**, C2084-2094 (2007); published online EpubJun (10.1152/ajpcell.00523.2006).
125. K. Haghighi, T. Pritchard, J. Bossuyt, J. R. Waggoner, Q. Yuan, G. C. Fan, H. Osinska, A. Anjak, J. Rubinstein, J. Robbins, D. M. Bers, E. G. Kranias, The human phospholamban Arg14-deletion mutant localizes to plasma membrane and interacts with the Na/K-ATPase. *Journal of molecular and cellular cardiology* **52**, 773-782 (2012); published online EpubMar (10.1016/j.yjmcc.2011.11.012).
126. Y. A. Chiou, Y. L. Sung, P. S. Chen, S. F. Lin, Z. H. Chen, Unique Localization of Phospholamban in Perinuclear Membranes of Cardiomyocytes from Several Species. *Biophysical journal* **110**, 122A-122A (2016); published online EpubFeb 16 (
127. A. C. Teng, T. Miyake, S. Yokoe, L. Zhang, L. M. Rezende, Jr., P. Sharma, D. H. MacLennan, P. P. Liu, A. O. Gramolini, Metformin increases degradation of phospholamban via autophagy in cardiomyocytes. *Proceedings of the National Academy of Sciences of the United States of America* **112**, 7165-7170 (2015); published online EpubJun 9 (10.1073/pnas.1508815112).
128. B. Levine, G. Kroemer, Autophagy in the pathogenesis of disease. *Cell* **132**, 27-42 (2008); published online EpubJan 11 (10.1016/j.cell.2007.12.018).
129. K. M. Fetalvero, Y. Yu, M. Goetschkes, G. Liang, R. A. Valdez, T. Gould, E. Triantafellow, S. Bergling, J. Loureiro, J. Eash, V. Lin, J. A. Porter, P. M. Finan, K. Walsh, Y. Yang, X. Mao, L. O. Murphy, Defective autophagy and mTORC1 signaling in myotubularin null mice. *Molecular and cellular biology* **33**, 98-110 (2013); published online EpubJan (10.1128/MCB.01075-12).
130. A. C. Durieux, S. Vassilopoulos, J. Laine, B. Fraysse, L. Brinas, B. Prudhon, J. Castells, D. Freyssenet, G. Bonne, P. Guicheney, M. Bitoun, A centronuclear myopathy--dynamin 2 mutation impairs autophagy in mice. *Traffic* **13**, 869-879 (2012); published online EpubJun (10.1111/j.1600-0854.2012.01348.x).

Appendix

Genotyping Protocol

All $\underline{\text{Pln}^{OE}}$ mice were ear notched and tagged at 3-4 weeks of age. The DNA was then extracted from ear notches samples using a pureLink Genomic DNA mini kit (Invitrogen, Carslbad, CA). PCR was performed on these DNA samples to amplify the DNA of interest. Briefly, approximately 50 ng of DNA was added to a Taq DNA polymerase mix (EP0402, Thermo Scientific Fermentas, Canada) containing Taq Buffer with (NH4)2S04 buffer (diluted to 1X), 4 mM MgCl2, 200 μM dNTP (R0192, Thermo Scientific Fermetas), 0.625 units of Taq DNA polymerase, and 0.4 μM of the appropriate forward and reverse primers (listed below). Samples were then placed in a thermal cycler (MJ MINI, Bio- Rad Canada) and underwent their respective PCR reactions (protocol below). The amplified products were then separated on a 1% agarose gel (in 1X TBE) containing 0.01% ethidium bromide (Bioshop, Canada) for 40 min at 80V in 1xTBE buffer, and identified using a bio- imaging system (Syngene, Frederick, MD).

Forward Pln^{OE} primer, SK-1 5'-AAG GGG CGG GAA GGC ATA TAG-3'
Reverse Pln^{OE} primer, PLB-RC 5'-GAT TCT GAC GTG CTT GCT GAGG-3'

***Pln^{OE}* PCR Protocol**

1. Denaturation @95°C for 3min
2. Denaturation @94°C for 30sec
3. Annealing @70°C for 30sec
4. Extension @72°C for 1 min
   *Repeat Steps 2-4 for 34 cycles
5. Final Extension @72°C for 10min
6. Hold @4°C until electrophoresis

NFAT Immunofluorescence Protocol

1. Remove slides and air dry for 5 mins
2. Pat Pen around sections
3. Incubate in 4% paraformaldehyde (make fresh: 25ml dH2O + 3ml formaldehyde) on shaker for 10 min at RT.
4. Wash 3 times for 5 min in PBS in Columbia jar while on shaker (approx 220 rpm). Blot excess.
5. Permeablize with 0.5% Triton X-100 solution for 30 min at RT on shaker. Blot excess.
6. Wash 3 times for 5 min in PBS in Columbia jar while on shaker (approx 220 rpm). Blot excess.
7. block in 5% Goat Serum-PBS for 1 hour at room temperature.
8. Primary at a dilution of 1:50 overnight at 4°C in a humidified chamber.
    a. Add Dystrophin 1:100
9. Wash extensively with PBS 3 times 5 min in Columbia jar while on shaker.
10. Secondary fluorescent IgG1 antibody 1: 500 for 1hr at RT
    a. Dystrophin secondary 1:500 IgG2a

    ****If nuclear counterstaining is needed proceed as follows:

    a. While sections are washing make up DAPI stain. Protected from light by wrapping in foil.

    b. To make DAPI: dilute 10µl of 30µM working solution to 990µl PBS. Keep new diluted solution wrapped in foil until needed.

    c. Incubate sections in DAPI stain for 2 min while in the dark. Use 100uL of the diluted solution per slide/group of sections.

    d. Wash 3 times for 5 min in dark on shaker in new PBS.
11. Blot excess. Add 15uL of Prolong to each slide/group of sections and cover with a #1 coverslip. These coverslips are very thin; if two are stuck together a "hologram" will be seen in their surfaces.
12. Carefully cover edges of coverslip with clear nail polish, and allow to dry in the dark for 5-10 minutes.

Primary Info
Catalog number: MA3-024
Company: ThermoFisher
Class: monoclonal
Host: Mouse
Isotype: IgG1
IF concentration: 1:10-100
IHC concentration: 1:20-200
Western blot: 1:2000
Secondary Info
IgG1

Counter Stain
DAPI – nuclei
Dystrophin (primary 1:100, secondary 1:500 IgG2a)

Western Blotting Protocols

Target Protein	Antibody Info	Total Protein Load	Run	Primary	Secondary	Detection
PLN	Pierce Antibodies MA3-922 Monoclonal Mouse	2.5ug	75 mins @100V	1:2000 signal enhancer 1hr at RT	1:2000 anti-mouse	ECL 30 sec exposure
CnA	Sigma Aldrich C1956 Monoclonal Mouse	10ug	15mins @120V,60 mins @100V	1:1000 5%milk in TBST overnight 4°C	1:2000	Femto 30 sec exposure
NFAT-p	Pierce Antibodies PA5-38301 Polyclonal Rabbit	20ug	15mins @120V,60 mins @100V	1:2000 5%milk overnight at 4°C in TBST	1:2000	Luminata 1 min exposure
NFAT	Pierce Antibodies MA3-024 Monoclonal Mouse	Strip and reprobe NFAT-p membrane		1:2000 signal enhancer overnight 4°C	1:2000	Luminata 1 min exposure
SLN	Lampire Biological Laboratories Proprietary Polyclonal Rabbit	20ug	75 mins @100V	1:100 3%BSA and TBST overnight 4°C	1:2000 anti-rabbit	Luminata 1 min exposure
Actin	Sigma Aldrich A2066 Polyclonal Rabbit	Strip and reprobe from different membrane		1:10000 5%milk in TBST 1hr at RT	1:2000	ECL 10 sec exposure